



1 **Formation and dynamics of sandy dunes in the inland areas of the Hexi Corridor**

2

3 Bing-Qi Zhu

4 Key Laboratory of Water Cycle and Related Land Surface Processes, Institute of Geographic Sciences and

5 Natural Resources Research, CAS, Beijing 100101, China

6

7 **Abstract:**

8

9 Dynamic changes of aeolian landforms and desertification under global warming in a middle-latitude
10 desert belt, the Hexi Corridor in China, considered to be one of the source and engine area of sandstorms
11 in China and Northern Hemisphere (NH), is a typical problem of climate change and landscape response,
12 which need a comprehensive understanding of the history and forcing mechanisms of recent landform and
13 environmental changes in the region. Based on the existing high-resolution satellite image interpretations,
14 field investigations and observations, comprehensive evidences from geomorphological, aeolian-physical,
15 granulometrical and geochemical analysis, this study discussed the formation of dune landforms, the
16 mechanism of desertification and their environmental implications in the Hexi Corridor. The analytical
17 results show that 80% of the sand particles flow within a height of 20~30 cm near the surface, and about
18 half of the sand particles flow within a height of 0.3~0.5 cm near the surface in the Hexi Corridor. The
19 average height of the typical crescent-shaped dunes is about 6.75m, and the minimum and maximum
20 values are between 2.6 and 11.2m. On the inter-annual and multi-year time scales, only the
21 crescent-shaped dunes and chains of barchan dunes are moving or wigwagging in the study area, while the
22 parabolic and longitudinal dunes did not move. Under the influence of wind speed, strong wind days and
23 other factors, the dunes at the edge of the Minqin Oasis move the fastest, with a moving speed of about
24 6.2m/a. Affected by the main wind direction and other factors, the dunes at the edge of the Dunhuang
25 Oasis move the slowest, with a moving speed of about 0.8m/a. The main factors affecting the dynamic
26 changes of sandy dunes in the Hexi Corridor are the annual precipitation, the annual average wind speed
27 and the number of annual strong wind days, of which the annual precipitation contributes the largest,
28 indicating that the climate factors have a most important impact on the dynamic change of sand dunes.
29 The cumulative curve of particle size frequency of dune sediments in the Hexi Corridor basically presents a
30 three-segment model, indicating a saltation mode dominated under the action of wind, but superimposed
31 with a small amount of coarser and finer particles dominated by the creeping and suspension models,
32 which is obviously different from that of the Gobi sediments with a dominant two-segment mode. The
33 palaeo-geographical, sedimentological and geochemical evidences indicate that dune sediments in the
34 Hexi Corridor are mainly derived from "locally or in-situ raised sandy sediments", which are mainly come
35 from alluvial plains and ancient fluvial sediments, as well as ancient lake plains and lacustrine deposits,



36 aeolian deposits in the piedmont denudation zones of the north and south mountains and modern fluvial
37 sediments in the corridor. In geochemical compositions of major and trace elements, the dunes in the Hexi
38 Corridor have certain similarities and differences to other sandy dunes in the northwest and northern
39 deserts of China or aeolian loess in the Loess Plateau. Sandy dunes in the Hexi Corridor are relatively rich
40 in iron and Co. Considering the proportion of fine particles on the surface, the coverage rate of surface salt
41 crust, and the potential migration of erodible sandy materials, it can be concluded that the Gobi area in
42 the west Hexi Corridor is not the main source area of sandstorms in the middle and east of the corridor,
43 but the north probably is. In the past half century, the warming and humidification of local climate is the
44 main cause of the reduction of sandstorms in the study area, and the Hexi Corridor has a potential trend of
45 anti-desertification, which is mainly controlled by climate change but not human activities. For the oasis
46 areas of the corridor, however, the effective measures to restrict desertification depend on human
47 activities. Restriction of the decline of groundwater is the key to preventing desertification in oases, rather
48 than water transfer from outer river basins.

49

50

51 **Keywords:**

52 Sandy dunes; Geomorphology; Sedimentology; Geochemistry; Desertification; Hexi Corridor.

53

54 **1. Introduction**

55

56 Aeolian sediments and their sedimentary strata record the environmental changes in the source areas
57 or desert areas and their responses to global climate change and human activities. They are unique and
58 important sedimentary and geomorphological archives of dryland landscape evolution (Goudie, 2002;
59 Lancaster et al. , 2013, 2016; Williams, 2014; Yang et al., 2019). In China, about 566,000 square kilometers
60 of land area are covered by aeolian sand, covering a wide range of geomorphological and tectonic
61 backgrounds ranging from 155m below sea level to 5,000m above sea level (Yang, 2006). The desert
62 landscapes dominated by active sandy dunes are mainly distributed in the arid areas with an average
63 annual precipitation of less than 200 mm, while the sandy-land landscapes dominated by semi-active
64 dunes and vegetated dunes mainly appeared in the semi-arid areas with an average annual precipitation of
65 200-400 mm (Zhu et al., 1980). The present geomorphology of these sandy deserts is the product of
66 long-term and short-term changes of the interaction between endogenic forces (such as tectonic
67 movement) and external forces (such as climate) of the earth system. In turn, these deserts may directly
68 affect the global climate system through sediment circulation (such as dust cycles) (Yang, 2006). Therefore,
69 the understanding of desert landscape evolution will increase our understanding of the earth system.

70 Regarding the formation and evolution of desert landscapes in China, the loess-paleosol sedimentary



71 sequences from the Loess Plateau indicate that the deserts in northwest China may have existed as early
72 as 22 myr (Guo et al., 2002, 2004), but the geomorphological and sedimentological evidences found inside
73 these deserts indicate that the modern-scale landscapes of these deserts are much younger in age (Yang et
74 al., 2004, 2006). But up to now, due to the lack of long-enough and continuous stratigraphic profiles, the
75 geomorphological connection between the Tertiary desert and the present desert is still unclear. And in
76 many areas of the deserts in northwest China, lacustrine and fluvial sediments from the Late Pleistocene
77 and even Holocene are buried under the sandy dunes, which indicate that the environment of these desert
78 areas has changed dramatically during the late Quaternary (Yang, 2006; Chen et al., 2020). For example, in
79 the Badanjin Desert near the northeast of the Hexi Corridor in China, although the formation mechanism
80 of the giant sandy dunes in the desert is still a dispute in people's understanding, such as "the theory of
81 climate control", "the theory of tectonical/geomorphological control" and "the theory of groundwater
82 control", geomorphological survey is essential to resolve this dispute. It is conceivable that the dynamic
83 genesis of sand dunes, namely desertification, will be crucial for understanding this problem, where the
84 dune landforms and desertification processes cover almost all the important information archives that
85 understanding the earth system.

86 The movement of aeolian materials and related formation, dynamics and evolution of dune landforms
87 are the results of the transportation and accumulation of sandy sediments under the influence of climate
88 (especially wind and atmospheric circulation), which is the direct cause of landsurface desertification and
89 one of its important manifestations (Zhu et al., 1980; Zhu and Wang, 1992; Yang et al., 2004, 2019). For
90 example, the ruins of ancient cities are buried by shifting sands in northern China and some famous
91 steppes in history but are occupied at present by desert landscapes with undulating sandy dunes, which
92 are clear evidences of land desertification in the past 2 Ka (Zhu and Wang, 1992). The movement of sand
93 dunes not only affects the development and safety of agriculture and transportation, but also reflects the
94 modern geomorphological processes of landform development in arid areas and its environmental
95 response to global changes. Therefore, it is of great significance to study the formation and dynamic
96 characteristics of various dune landforms in different regions of the world to reveal desertification and
97 environmental changes in drylands.

98 The formation and dynamics of sandy dunes in the world were observed and studied for the first time
99 in the United States (Finkel, 1959) and the former Soviet Union (Znamenski, 1962) in the 1950s. During this
100 period, the famous desert physicist Bagnold put forward the formation mechanism of mobile sandy dunes
101 and the formula of moving velocity of active dunes (Bagnold, 1959). Dune formation and dynamics in
102 China were qualitatively or semi-quantitatively described in most early studies (Yang, 2006). For example,
103 some pioneer scholars have studied the development and movement of sandy dunes in the Taklamakan
104 Desert, and they quantitatively analyzed the moving speed and evolution process of local crescent sandy
105 dunes (Zhu et al., 1964; Zhu et al., 1980, 1981). However, these studies still laid a solid foundation for the



106 later development of refined and quantitative researches due to the progress of research methods and
107 technical tools, and they are still a milestone cornerstone of desert researches in China.

108 The Hexi Corridor in northwestern China at the middle-latitudes of Northern Hemisphere (NH) was
109 once one of the most important trunk sections of the world-famous Silk Road, and also a place where
110 several ancient cultures converged. However, today it is facing severe problems of desertification and
111 climate change under global warming. For nearly half a century, frequent sandstorms in northern China
112 have been considered to be the notorious tragedy and direct consequence of the desertification in the
113 Hexi Corridor, because the Hexi area is considered to be the main source area and the engine area of
114 sandstorms in China (Zhang and Ren, 2003; Pu, 2005; Li and Zhang, 2007). Therefore, the problem of
115 desertification in the Hexi Corridor is one of the major problems that have been urgently needed to be
116 resolved in Gansu Province and even in northern China for half a century.

117 The purpose of this study is, based on the comprehensive evidences from the extensive dune
118 geomorphological survey, the sedimentological and geochemical analysis of dune sediments, and the
119 meteorological analysis of local weather records in the past several decades, to understand the genesis
120 and dynamic changes of sandy dunes in the Hexi Corridor and its relationship with climate change during
121 the past half century, and to explore the mechanism of local desertification in the Hexi Corridor and its
122 environmental implications.

123

124 **2. Background and analytical methods**

125

126 **2.1. Geographical, geological, geomorphological and hydrological backgrounds of the Hexi Corridor**

127

128 The Hexi Corridor is located in the central and western parts of Gansu Province in Northwest China
129 (Fig.1), including Wuwei, Jinchang, Zhangye, Jiuquan, Jiayuguan and other cities in the west of the Yellow
130 River, with a total area of approximately 5,100 square kilometers. In terms of regional geomorphology, the
131 Hexi Corridor is located in the lowland area between the Qilian Mountains and the Alashan Plateau. The
132 Alashan Plateau in the north of the Hexi Corridor distributes three large sandy deserts of China, i.e. the
133 Badanjilin Desert, the Tenggeli Desert and the Ulanbuhe Desert. For the Qilian Mountains in the south of
134 the Hexi Corridor, the melting water of ice and snow in the Qilian Mountains in the south converges into
135 several large rivers flowing northward into the Hexi Corridor, such as the Heihe River, the Shiyang River and
136 the Shule River, etc. In the middle and lower reaches of these rivers flowing through the south corridor,
137 diluvial and alluvial fans are well developed, and hydrologically, they are also the main locations of spring
138 overflow zone of each catchment derived from the Qilan Mountains. Oases are widely developed in the
139 toes of these alluvial fans and are the major agricultural exploitation areas and the resident agglomeration
140 areas of northwest China.



141 In climate, the Hexi Corridor is located in the center of temperate desert belt in the mid-latitudes of
142 Northern Hemisphere. Except for the forest and grasslands distributed in the middle- and high-elevation
143 mountain areas in the south, most of the Hexi Corridor is under a typical arid desert climate with desert
144 landforms developed. The desert types are dominated by Gobi desert and sandy desert, which account for
145 46.64% of the total area of the region.

146 In history, the Hexi Corridor was a necessary place for the famous ancient Silk Road in China. In
147 modern times, however, the expansion of population and socio-economic development of the Hexi
148 Corridor, as well as the human-caused competitive redistribution of water resources, have led to the onset
149 and enhancement of desertification in the Hexi Corridor (Pu, 2005). The expansions of sandy dunes and
150 dune fields in the corridor, and even the combination with surrounding sandy desert, have occurred in the
151 past 2 ka (Zhu and Wang, 1992; Ren et al., 2014).

152 In terms of aeolian landforms, sands dunes or dune fields in the Hexi Corridor are mainly distributed
153 in a narrow and long belt between the Qilian Mountains and the Heli mountains to the west of Wushaoling
154 and the east of Palaeo-Yumenguan (Fig. 2) (Zhu et al., 1980). Compared with the dune landforms in the
155 adjacent areas of the Badanjilin and Tenggeli Deserts, the sandy dunes in the two deserts tend to be
156 convergent in spatial distribution, while the Hexi Corridor is different, where the dunes are almost
157 scattered, mainly distributed in the vicinity of oases along some rivers, in the oasis or Gobi desert areas
158 (Fig. 2). From east to west in the dune belt, sand dunes are mainly distributed around the Minqin Oasis in
159 the lower reaches of the Shiyang River, the Zhangye and Gaotai oases in the middle reaches of Heihe River,
160 the Jiuquan and Jinta oases in the lower reaches of the Beidahe River, and the Dunhuang oasis in the lower
161 reaches of the Danghe River (Fig. 2) (Zhu et al., 1980).

162 The total area of dune fields in the Hexi Corridor is about 754 square kilometers, and a large number
163 of big crescent-shaped dunes and chains of crescent-shaped dunes develop on the edges of oases. The
164 Minqin Basin is a typical area with dune landforms development in the Hexi Corridor. It is located at the
165 lower reaches of the Shiyang River and the western edge of the Tenggeli Desert. The annual average
166 precipitation is about 116.4 mm and the annual average wind speed is about 2.25 m/s. A large number of
167 crescent-shaped sandy dunes are distributed on the northwestern edge of the oasis, i.e., the windward of
168 sand-transport winds in the oasis.

169

170 **2. 2. Data and analytical methods**

171

172 For the study of sandy dune geomorphology, the first method is to use the sample-quadrant survey
173 procedure to measure the height and shape of typical high dunes in the field with a rangefinder, and the
174 second is to measure the length, angle and width of the windward slope and downwind slope of each
175 dune in the sample quadrant and between different quadrates along the local dominant wind direction by



176 using rangefinder and remote sensing image scales (such as Google Earth scales, etc.), and then the
177 comprehensive geomorphic data of sandy dunes in the region is obtained. In addition to the
178 geomorphological data of sandy dunes themselves, landscape researchers will also use the
179 sample-quadrature survey method to investigate the ecological parameters of vegetation cover in the
180 selected sampling area. For both geomorphological and ecological surveys, sub-scale sample quadrates will
181 be selected from the upper, middle and lower parts of the windward and leeward slopes of each dune.
182 Three quadrates can be selected from the dune slope in the windward and downwind directions of each
183 dune along the local prevailing wind direction and the size of each quadrate can be designed as 5m × 5m
184 or smaller (Chang et al., 2016a, 2017; Lang et al., 2017).

185 In recent years, a number of studies have been systematically carried out in different areas of the Hexi
186 Corridor to investigate the different landform types of widespread sandy dunes at a geomorphic unit scale
187 in the field, including the crescent-shaped (barchan) dunes, chains of barchan dunes, pyramid-shaped
188 dunes, parabolic dunes and longitudinal dunes belt. Based on field observations and satellite remote
189 sensing image data in different periods, the geomorphological parameters and characteristics of these
190 dunes are obtained (Zhang and Dong, 2014; Chang et al., 2016a, 2017; Lang et al., 2017). The
191 geomorphological parameters of part of these dunes in the Hexi Corridor and their comprehensive data
192 are shown in Tables 1 and 2.

193 In addition to the above-mentioned intuitive survey and measurement of geomorphic parameter of
194 sandy dunes, quantifying the structure of wind-blown sand flow and the movement rate of dunes is also
195 the most direct and effective means to explain the dynamic change of dunes and their geomorphological
196 evolution (Dong et al., 1998; Chen and Liu, 2011; He et al., 2012; Dong and Huang, 2013; Wang et al., 2013;
197 Hu et al., 2016; Mao et al., 2016). Generally, there are two methods to study the moving velocity of sandy
198 dunes, one is early positioning observation (MDCES, 1975; Dong et al., 1998; He et al., 2012) and the other
199 is based on remote sensing images (Chen and Liu, 2011; Dong and Huang, 2013; Mao et al., 2016).
200 Research works based on the both methods have been carried out in dune fields of the Hexi Corridor. On
201 this basis, this study will integrate and organize the different observation data of dune movement
202 measurement in the Hexi Corridor, and further discuss the geomorphological evolution of sandy dunes in
203 the Hexi corridor.

204 The grain size composition and distribution of aeolian sediment is an important indicator to
205 understand the formation and development of sand dunes. This is because the grain size parameters of
206 sand particles can be used not only to distinguish the depositional environment (aeolian, fluvial or
207 lacustrine), but also to identify the movement types (creep, saltation or suspension) of sediments in the
208 transportation process. Therefore, the analysis and study on the granular sedimentology of sandy dunes is
209 a basic method to understand the genesis and evolution of the dunes in the Hexi Corridor. At present,
210 research works about the grain-size sedimentology of aeolian sediments and related aqueous sediments,



211 such as alluvial and proluvial fans, lacustrine deposits, fluvial deposits, has been widely carried out in the
212 Hexi Corridor (Zhu and Yu, 2014; Zhu et al., 2014; Zhang and Dong, 2015; Zhang et al., 2016; Pan et al.,
213 2019; Zhang et al., 2020). On this basis, this study systematically collects and organizes the granular
214 evidences, which makes it possible to conduct a comprehensive and comparative study on the dunes in
215 the Hexi Corridor from a perspective of sedimentology.

216 Erodible clastic sediments as the material sources are the fundamental base for the formation of
217 sedimentary landforms (Pettijohn et al., 1972; Taylor and McLennan, 1985). Therefore, identifying the
218 source of wind-induced materials in an arid environment is a prerequisite for understanding the formation
219 of dune landforms (Zhu et al., 1980, 1981; Yang et al., 2012). The analysis of major and trace elements,
220 including rare earth elements, has become a reliable technique for detecting the source of desert
221 sediments (Muhs et al., 1995, 1996; Pease et al., 1998; Honda and Shimizu, 1998; Wolfe et al., 2000; Pease
222 and Tchakerian, 2003; Zimelman and Williams, 2002; Muhs, 2004; Yang et al., 2007; Zhu and Yang, 2009;
223 Jiang and Yang, 2019). The reason is that for aeolian sediments, the differences in compositions and
224 distributions of rare earth elements and other trace elements in different samples/sub-fractions are largely
225 controlled by the parent-rock compositions, because these elements only exist in specific minerals and are
226 difficult to be lost during transportation (Pettijohn et al., 1972; Taylor and McLennan, 1985). In the Hexi
227 Corridor, preliminary results have been achieved in the case studies of analyzing the elemental
228 compositions of aeolian sediments using major- and trace-element geochemical methods (e.g., Ren et al.,
229 2014; Pan et al., 2019; Zhang et al., 2020), which provide basic data for this study to comprehensively
230 identify the material sources of different dunes in the study area.

231 The continuous data records of different meteorological parameters of local weather stations in the
232 Hexi Corridor in the past half century, such as temperature, precipitation, relative humidity, wind speed,
233 strong wind days and sandstorms days, will not only be the basis for this study to discuss the regional
234 climate change under the background of global warming, but also the basis for exploring the response of
235 regional landscape to climate change based on the statistical relationship between geomorphic parameters
236 and climate parameters on a multi-decade time scale. Therefore, this study will collect and use the
237 meteorological data of the Hexi Corridor for nearly half a century to analyze the regional climate change
238 and its relationship with the dynamic changes of dune landforms.

239

240 **3. Results**

241

242 **3.1. Geomorphological parameters (Height, shape, and dynamics) of sandy dunes in the Hexi Corridor**

243

244 The comprehensive data on the heights of different types of sandy dunes widely developed in
245 different areas of the Hexi Corridor, as well as other geomorphic parameters of these dunes, can be found



246 in Table 1, Table 2 and Fig. 3. It can be seen from Table 1, Table 2 and Fig. 3 that the average height of
247 typical crescent-shape (barchan) dunes in the Hexi Corridor is about 6.75m, the maximum is about 11.20m,
248 and the minimum is only about 2.60 m. The average height of typical chains of barchan dunes in the study
249 area is about 9.23 m, the maximum is about 13.80 m, and the minimum is only about 5.80 m. The typical
250 pyramid-shaped dunes in the study area have an average height of about 86.25 m, with a maximum of
251 about 121.80 m and a minimum of about 25.80 m. The average height of typical parabolic dunes in the
252 study area is about 4.08 m, the maximum is about 4.60 m, and the minimum is only about 3.38 m. The
253 average height of typical longitudinal dunes in the study area is about 13.02 m, the maximum is about
254 18.60 m, and the minimum is only about 5.60 m.

255 Regarding the dynamic changes of sandy dune landforms, as early as 1959-1964, the newly
256 established Minqin Comprehensive Experimental Station of Desertification Control (MCESDC) in China
257 carried out the field positioning observation and research on wind-blown sand flows in the Hexi Corridor
258 (Zhu et al., 1980; Zhu, 1994, 1999; Zhu and Wang, 1992; Wang, 2003). For example, 187 positioning
259 observation points were set up in field along a 20km long observation line in the Minqin Basin and a large
260 number of observations were made to assess the structure of wind-blown sand flow, the shape of sand
261 dunes, erosion and accumulation of aeolian sand, changes in sand ripples and sand dune movement, etc.
262 Later works continued to carry out relevant researches on different areas of the Hexi Corridor (MDCES,
263 1975; Zhu et al., 1980; Wang, 2003; Zhang et al., 2004; Qu et al., 2005; Wang et al., 2013; Yin et al., 2014,
264 2016; Chang et al., 2016a, 2017; Zhang et al., 2016; An et al., 2019; Chang, 2019; Hu et al., 2020). Results
265 of these studies show that in the Hexi Corridor, 80% of the sand particles of the wind-blown sand flows are
266 moving in the height of 20 ~ 30cm near the ground surface, of which about half of the sand particles are
267 moving in the height of 0.3 ~ 0.5cm near the surface. At the wind speed of 7m/s, 75% of the sand particles
268 are within the height of 10cm, and only 0.035% are within the height of 76 ~ 200cm. The movement
269 modes of sand particles in the Hexi Corridor include creeping (wriggling/rolling), saltation
270 (jumping/springing) and suspension (floating/levitating), and the movement modes of sandy dunes
271 include three ways: straight-forward movement, wigwagging movement, and onward-wigwagging
272 movement (Wang, 2003).

273 Among the different sandy dunes in the Hexi Corridor, the crescent-shaped (barchan) dunes, chains of
274 barchan dunes, pyramid-shaped dunes, parabolic dunes and longitudinal dunes have received the most
275 extensive attention. Based on field surveys/measurements (e.g. measurement of the electronic total
276 station) and satellite image (e.g. Google Earth) data of different periods, the researchers obtained the
277 geomorphological parameters and moving speeds of these different dunes (e.g. Ren et al., 2010; Chang et
278 al., 2016a), as shown in Table 1 and Fig. 3.

279 It can be seen that the average moving speed of the crescent-shaped dunes is about 6.62 m/a, the
280 maximum is 12.51 m/a, and the minimum is only 1.01 m/a (Fig. 3a). The average moving speed of the



281 chains of barchan dunes is about 6.54 m/a, the maximum is 8.30 m/a, and the minimum is only 5.34 m/a
282 (Fig. 3b). Compared with the crescent-shaped dunes, the chains of barchan dunes move relatively slowly
283 and the movement speed changes little. In general, the crescent-shaped dunes and the chains of barchan
284 dunes in the Hexi Corridor move along the NW-SE direction. The direction of movement of the east part of
285 the corridor is about N45° W, while the movement angle of the Jinta area in the western corridor increases
286 (Table 1 and Fig. 3). The average swing velocity at the tops of the pyramid dunes is about 6.32 m/a, the
287 maximum is 97.37 m/a, and the minimum is only 1.14 m/a. The direction of movement of the pyramid
288 dunes will also change, but its main direction of motion is SW-NE (Fig. 3).

289

290 **3. 2. Granular sedimentology of sandy dunes in the Hexi Corridor**

291

292 In the Jiuquan Gaotai area in the middle and Eastern Hexi Corridor (area B in Fig. 2), grain size
293 parameters (including mean, standard deviation, skewness and kurtosis, etc.) of sand dunes at different
294 geomorphological positions on the dune surface, such as the toes of windward slope, slope surface, dune
295 crest (top), toes of leeward slope, were determined (Zhang and Dong, 2015). The granular sedimentology
296 shows that the grain-size frequency cumulative curves of sand dunes in this area are mostly unimodal, and
297 a few are bimodal (Fig. 4); the dune surface sediments are mostly fine sand fraction and very fine sand
298 fraction, with an average grain size of $0.07\text{ mm} \pm 0.01 \sim 0.24\text{ mm} \pm 0.06$, which is similar to the average
299 particle size of sand dunes in the world. The finer the dune particle is, the better the sorting degree is. The
300 mean grain size increases with the increase of the skewness values, but decreases with the increase of the
301 kurtosis values. From upwind to downwind, the dune sediment becomes finer, the medium-sand fraction
302 decreases, and the fine-sand fraction, very-fine-sand fraction, silt-fraction and clay-fraction increase; the
303 source materials affect the changes in the average grain size of dune sediment from upwind to downwind
304 (Zhang and Dong, 2015). In this dune field, there are three types of grain-size-distribution patterns in a
305 dune-scale unit: the dune crest is coarser (the dune slope and inter-dune area are finer), the dune crest is
306 finer (the dune slope and inter-dune land are coarser), and there is no significant difference between dune
307 crest, windward and leeward slopes. Among them, the coarser-dune-crest model is the most common type,
308 accounting for 69% of all sandy dunes, while the finer-dune-crest is the second most common type
309 (accounting for 24%) (Zhang and Dong, 2015).

310 In the Jinta-Jiayuguan-Huahai area in the western Hexi Corridor (area A in Fig. 2), the crescent-shaped
311 (barchan) dunes developed on the Gobi desert and ancient playas have been systematically studied on
312 granular sedimentology (Pan et al., 2019). The results of this research show that the grain size of the
313 surface aeolian sediments of crescent-shaped dunes in the western Hexi Corridor is mainly the
314 medium-sand fraction (21.7~57.4%), followed by the fine-sand fraction (23.2~53.0%); the mean grain



315 size ranges between 0.27~0.43 mm (while the paleolacustrine sediment ranges between 0.10~0.21 mm)
316 (Pan et al., 2019). The crescent-shaped dune sediments in this region are mainly medium to good in the
317 sorting level. The frequency cumulative curves of dunes are mostly unimodal and nearly symmetrical, and
318 the kurtosis is medium in level. The granular characteristics of sand dunes in this region are closely linked
319 to their dune morphology and the properties of the underlying Gobi surface (Pan et al., 2019).

320

321 **3. 3. Geochemical and sources of dune sediments in the Hexi Corridor**

322

323 Regarding the source of aeolian sediments, the provenance of sandy dunes in the Hexi Corridor was
324 firstly investigated as early as 1959-1964 by the China's Minqin Comprehensive Experimental Station of
325 Desertification Control (MCESDC) (MDCES, 1975; Zhu et al., 1980; Chang, 2019), and continues to this day
326 (Ferrat et al., 2011; Ren and Wang, 2010; Ren et al., 2014; Zhang and Dong, 2015; Zhang et al., 2016, 2020;
327 Chang, 2019).

328 Due to the application of geochemical methods in recent years, it is possible to identify sediment
329 sources more precisely (Wang, 2011; Wang and Wang, 2013; Ren et al., 2014; Pan et al., 2019; Zhang et al.,
330 2020). In this study, based on geochemical evidences, we take the Gobi areas in the Huahai-Jiayuguan-Jinta
331 region of the west Hexi Corridor (area A in Fig. 2), the Jinta-Gaotai region of the middle Hexi Corridor (area
332 B in Fig. 2) and the Minqin Basin in the east Hexi Corridor (area C in Fig. 2) as the case examples (Ren et al.,
333 2014; Pan et al., 2019; Zhang et al., 2020) to explore the material sources of sandy dunes developed in
334 these regions.

335 The Minqin Basin is dominated by an oasis landscape. It is located in the east Hexi Corridor (area C in
336 Fig. 2), and the northern edge of the Loess Plateau, and is bordered by the Badanjilin Desert to the
337 northwest and the Tenggeli Desert to the southeast (Figs. 1 and 2). The Minqin Basin is considered a
338 natural obstacle to the convergence of the two deserts (Zhu et al., 1980). Geographically and
339 geomorphologically, identifying the origin and transportation of aeolian sediments in the Minqin oasis and
340 its adjacent desert areas will help to better understand the relationship between loess and desert in China
341 (Liu, 1985; Sun, 2002; Yang et al., 2007a; Yang et al., 2011; Ren et al., 2014).

342 The research works of Ren et al., (2014) and others (Ren, 2010; Ren and Wang, 2010) systematically
343 collected aeolian sediment samples from sandy dunes in the Minqin Oasis and its surrounding desert areas.
344 Through geochemical analysis, combined with wind data and cluster analysis methods, the characteristics
345 of compositions and spatial distributions of major and trace elements of aeolian samples from the Minqin
346 Oasis and its adjacent deserts (the Badanjilin and Tenggeli Deserts), as well as the provenance and
347 transportation pathways of aeolian sediments in these areas, were discussed. The analysis of geochemical
348 data shows that in the bulk (whole-rock) samples of sandy dunes in the Minqin Basin (M) and its



349 surrounding areas (the Badanjilin Desert B, the Badanjilin-Minqin transition zone BM, the Tenggeli-Minqin
350 transition zone TM, the northeast edge of the Tenggeli Desert TNE, the southwest edge of the Tenggeli
351 Desert TSW), the contents of major elements are higher in the content of SiO_2 , reaching between 72.2%
352 and 88.9% with an average of about 83.3%. In contrast, the contents of most trace elements are relatively
353 low, and only the contents of Ba, Ce, Co, Mn and Sr reach > 100 ppm (Ren, 2010; Ren et al., 2014).
354 Compared with the average composition of the upper continental crust (UCC, Taylor and McLennan, 1985),
355 the concentrations of Ba, SiO_2 , Rb, Sr, Al_2O_3 and K_2O in the Minqin Basin and its surrounding areas are
356 relatively uniform (Fig. 5), indicating that the spatial differences of these elements in abundance are small
357 and they are relatively homogeneous in the study area, while obvious convex and concave shapes are
358 observed for other elements (Fig. 5), indicating that the spatial differences of these elements in
359 abundances are large and they are relatively heterogeneous in the study area. The homogeneous and
360 heterogeneous characteristics between different elements thus can be used as geochemical indicators to
361 identify different sources of sediments in the study area. For the major elements' compositions, only SiO_2
362 is enriched relative to UCC, and the others are relatively depleted (Fig. 5). For the trace elements'
363 abundance, most elements are depleted, except for Cr and Ni enriched in B and BM area and Cr enriched
364 in TNE area. The binary and ternary diagrams of some major and trace elements and their ratios, such as Cr,
365 Ni, Cr/V, Y/Ni, Al, V, Zr, Hf, Zr/Hf, reveal that sandy dunes have different material sources between the
366 western part of the Minqin Basin (including sub-area B, BM and TNE) and the southeast side of the Minqin
367 Basin (TSW), while sand dunes in the Minqin Basin (M) and the Tenggeli-Minqin transition zone (TM) are
368 related to the two big deserts, respectively (Ren et al., 2014).

369 Some researchers have conducted geochemical analysis of major and trace elements in aeolian
370 sediments of barchans dunes and other sediments developed in the western Hexi Corridor (Zhang et al.,
371 2017; Pan et al., 2019). The dunes studied are located in the Gobi area to the north and west of Jiayuguan
372 (area A in Fig. 2). The dune types are mainly barchan dunes, chains of barchan dune and asymmetric
373 barchans dunes (Zhang et al., 2017; Pan et al., 2019). The aeolian samples were mainly collected from the
374 surface sediments of barchan dunes and asymmetric barchan dunes, including different geomorphic sites
375 of dunes such as the crest of dune, the bottom of the windward slope, the middle of the windward slope,
376 and the bottom of the leeward slope. The analytical results show that after the standardization of UCC, the
377 barchan dunes on the Gobi surface in the western Hexi Corridor are significantly enriched in the major
378 elements CaO and SiO_2 (accounting for 5.55% and 66.12% of the total rock mass, respectively). The
379 element contents of CaO, MgO and Fe_2O_3 are gradually enriched from northwest to Southeast, that is, the
380 enrichment degree increases along the dominant wind direction. The UCC-normalized concentrations of
381 Na_2O and K_2O are both significantly <1 , indicating that alkali metal elements are significantly depleted or
382 leached in the study area (Zhang et al., 2017; Pan et al., 2019). The contents of trace elements vary among
383 different dune samples, reflecting a complexity of provenance of these dune sediments; however, the



384 variations of trace elements are similar in different geomorphic positions of the one dune (Pan et al., 2019).
385 Compared with UCC, trace elements Co, As, La, and Nd are significantly enriched, while other elements are
386 depleted. Compared with the chemical elements in the Tenggeli and Badanjilin Deserts (Li, 2011), the Hexi
387 Corridor has lower SiO₂ content, similar K₂O content, and lower contents of other trace elements.

388 Mineralogical and major- and trace-element geochemical analyses of aeolian sediments from the
389 Jinta-Gaotai area (area B in Fig. 2) in the middle Hexi Corridor have been carried out (Ferrat et al., 2011;
390 Wang and Wang, 2013; Wang et al., 2018; Zhang et al., 2020). These studies use the light/heavy mineral
391 assemblages, the ratios of Na₂O/Al₂O₃ to K₂O/Al₂O₃ and SiO₂/Al₂O₃, Ba/Sr to Rb/Sr, Rb/Sr to Ce/Sr, and the
392 composition of CaO and Cl to identify the provenance of aeolian sediments in the study area. Similar
393 mineralogical compositions (mica, quartz, illite, muscovite and albite) are found in dune sediments from
394 the Hexi Corridor and adjacent areas such as the Tenggeli and Badanjilin Deserts (Ferrat et al., 2011). This
395 feature is also found by major and trace element analysis (Wang and Wang, 2013; Zhang et al., 2020),
396 indicating that the geochemical characteristics of aeolian sediments in the Hexi Corridor and its adjacent
397 areas are also similar. Compared with the composition of the upper continental crust (UCC), dune
398 sediments in the Jinta-Gaotai area in the middle Hexi Corridor are also enriched in CaO (Fig. 6). Through
399 the methods of multi-dimensional scaling (MDS), principal component analysis (PCA) and regional
400 topography analysis, these studies suggest that the Hexi Corridor is not only the sediment sink of the Qilian
401 Mountains, but also the sediment sink of the Beishan Mountains. The sandy dunes from the Hexi Corridor
402 are similar in provenance to those from the Tenggelil, Badanjilin, and Kumtag Deserts (Zhang et al., 2020).

403

404 **4. Discussion**

405

406 **4. 1. Physiochemical characteristics of sandy dunes in the Hexi Corridor**

407

408 The above analytical results of geomorphological parameters indicate that in the dynamic process of
409 different dunes in the Hexi Corridor, the crescent-shaped dunes move the fastest, followed by the chains of
410 barchan dunes; only the top of the pyramid dunes wigwags, while the parabolic dunes and the longitudinal
411 dunes hardly move forward; the higher the height of the crescent-shaped dune (or the chain of barchan
412 dunes) is, the slower their movement is; on the contrary, the higher the height of the pyramid dunes is, the
413 faster they swing. Analysis also suggests that the moving speed of sandy dunes is positively correlated with
414 the average wind speed of sandstorms.

415 Here, we compare the moving speed of sandy dunes in the Hexi Corridor with that in other desert
416 areas in northwest China. For example, the observation results of eight crescent-shaped dunes along the
417 oil transportation highway in the Taklamakan Desert show that the moving speed of sandy dunes in
418 October 1991~1992 is 4.81~10.87 m, with an average of 7.29 m; the moving speed of sandy dunes in



419 October 1992~1993 is 3.33~8.89 m, with an average of 5.56 m (Dong et al., 1998). Regarding the
420 analytical results based on high-resolution remote sensing images in 2010~2014, the average speed of
421 dune movement in the Tenggelish Desert was 4.36 m/a in 2010~2013, and was 2.43 m/a in 2013~2014
422 (He et al., 2016). For the research about the movement of crescent-shaped dunes in the Maowusu Sandy
423 Land based on Google Earth images (Wang et al., 2013), the moving speed of sandy dunes in the study
424 area is between 3.5 and 9.5 m/a; the width of the dunes is significantly correlated with the horizontal
425 length of the leeward slope; the width of the dune and the horizontal length of the leeward slope decrease
426 during the movement of dunes, while the horizontal length of the windward slope increases; there is a
427 good correlation between the moving speed and the width of the dune.

428 Compared with the dynamic process of sandy dunes in different deserts mentioned above, the
429 crescent-shaped dunes widely distributed on the edge of oases in the Hexi Corridor also have obvious
430 spatial differences in dynamic changes. For example, during the period 2006~2015, due to the influence
431 of wind speed, strong wind days and other factors, the sandy dunes at the edge of the Oasis in the Minqin
432 area moved the fastest, with a moving speed of about 6.2m/a; affected by the main wind direction and
433 other factors, the sandy dunes at the edge of oasis in the Dunhuang area moved the slowest, with a
434 moving speed of about 0.8m/a; under the influence of different meteorological factors, the horizontal
435 length of the windward slope of sandy dunes in most areas of the Hexi Corridor increased in 2015
436 compared with 2016, while the horizontal length of the leeward slope decreased. There are three main
437 factors influencing the dynamic changes of sandy dunes in the Hexi Corridor, i.e. the annual precipitation,
438 the annual average wind speed, and the annual strong wind days, among which the annual precipitation
439 has the largest contribution rate (Shi et al., 2018). It can be concluded that meteorological factors (or
440 climate factors) have an important impact on the dynamic change of sandy dunes in the Hexi Corridor, and
441 this impact has both positive (promoting) and negative (inhibiting) effects.

442 The above analytical results of granular sedimentology of aeolian and aqueous sediments (alluvial and
443 proluvial fans, lacustrine and fluvial deposits, etc.) from the Hexi Corridor have shown that sand dunes
444 have different grain size compositions in different regions of the Hexi Corridor. This is also confirmed by
445 many previous works (Zhu and Yu, 2014; Zhu et al., 2014; Zhang and Dong, 2015; Zhang et al., 2016; Pan et
446 al., 2019; Zhang et al., 2020). The spatial differences in grain size compositions reflect the different
447 depositional environment, the different sources and the different transportation modes in the formation
448 and development of sandy dunes in the Hexi Corridor.

449 Based on the Sahu (1964) discriminant function, the sedimentary environment in the middle and
450 eastern part of the Hexi Corridor includes three types of deposits, i.e., aeolian deposit, lacustrine deposit
451 and alluvial-proluvial deposit, of which aeolian deposit is the dominant (about 50%) (Zhang and Dong,
452 2015).



453 It is obvious that the average grain size of sand dunes in of the western Hexi Corridor (such as the
454 Jiaquan-Jinta area) is larger than that in the central-eastern Hexi Corridor (such as the Jiuquan-Gaotai area)
455 and also larger than those in other desert regions of northern China. Compared with the crescent-shaped
456 dunes in the central-eastern Hexi Corridor, the top of shrub dunes in the western Hexi Corridor is
457 dominated by the medium- to fine-sand fractions, but not the medium-sand fraction. This is possibly
458 because of the wide distribution of gravel around the shrub dune, which reduce the airflow velocity near
459 the ground, making it difficult for the coarser-grained particles to move up to the surface of shrub dunes.
460 While for the crescent-shaped dunes, the length of wind flow path on the windward side of the dune is
461 longer. During the long-distance movement of the unsaturated aeolian sand flow, the coarser-grained
462 particles collide with the ground surface elastically, resulting in the coarser-grained particles moving to a
463 higher position on the windward slope of crescent-shaped dune, so the crescent-shaped dunes are
464 dominated by the medium-sand-fraction particles. The clay-grain content is less in the surface layer of
465 crescent-shaped dunes and shrub dunes, but more (up to 28.2%) in sandy dunes developed on dry lake
466 beds (playas) or ancient lake area, which is relevant to the local source of fine particles.

467 Generally speaking, the probability cumulative curve of grain size of aeolian sediments in the world is
468 usually shown as 2~4 independent line segments, indicating that 2~4 modes of motion occur during
469 their transportation (Visher, 1964). The probability cumulative curve of grain size of sandy dunes in the
470 Hexi Corridor basically presents a 3-stage pattern, indicating that the sandy dunes here are dominated by
471 the motion mode of saltation under the action of wind, and superimposed with a small amount of
472 particles transported by the motion modes of suspension and creeping. This feature has been observed in
473 sand dunes in different areas of the Hexi Corridor (Zhang and Dong, 2015; Zhang et al., 2016; Pan et al.,
474 2019), including the sand dunes in the lower reaches of the Heihe River Basin near the Hexi Corridor (Zhu
475 et al., 2014). But compared with dune sediments, the movement modes of Gobi sediments and lacustrine
476 sediments are mainly creeping-saltation and saltation-suspension, respectively (Zhu and Yu, 2014; Zhang et
477 al., 2016), indicating that the motion mode of lacustrine sediments and Gobi sediments is different from
478 that of dune sediments. This can also be reflected from the differences in the frequency accumulation
479 curves of dune sediments, Gobi sediments, and lacustrine and fluvial sediments in the Hexi Corridor (Fig.
480 4). Dune sediments are usually unimodal distribution, while aqueous sediments are usually bimodal or
481 multimodal distribution (Zhu, 2007; Zhu and Yu, 2014).

482 The above geochemical analysis provides good evidences for the understanding of the material
483 sources of sand dunes in the Hexi Corridor. The factor that sand dunes in the Minqin area have different
484 material sources between the western part (the Badanjilin-Minqin transition zone), the central part, the
485 southeast side, and the eastern part (the Tenggeji-Minqin transition zone) of the Minqin Basin indicate that
486 aeolian sediments from the Badanjilin Desert can be transported to the west side of the Minqin Oasis



487 through mountains (Yabulai) for a long distance by the northwest wind, and aeolian sediments from the
488 Tenggeli Desert provide sediment source to the east side of the Minqin Oasis. However, the aeolian
489 sediments of the two deserts cannot reach or bypass the other side of the Oasis (that is, not crossing the
490 oasis barrier to achieve a confluence of the two deserts). This study reveals that the Minqin Oasis is an
491 effective barrier to prevent the migration and convergence of sandy dunes between the Badanjilin and
492 Tenggeli Deserts. However, the large number of aeolian dunes developed in and around the Minqin Basin
493 also suggests that the role of oasis in preventing aeolian erosion is limited and should not be
494 overestimated.

495 Comparing the major element abundances of aeolian sediments in different deserts of China (Table 3),
496 the barchan dunes in the Hexi Corridor have certain differences and similarities with deserts in northwest
497 and north-central China. For example, the content of Fe_2O_3 in sand dunes of the Hexi Corridor can reach
498 3.50%, which is generally higher than any one of other deserts, while the contents of other elements in the
499 Hexi Corridor are in a similar range of element abundance to those of other deserts, indicating that the
500 sandy dunes in the Hexi Corridor are rich in iron element. Compared with the composition of the upper
501 continental crust (UCC), dune sediments in the middle and eastern Hexi Corridor are enriched in SiO_2 (Figs.
502 5-6) and CaO (Fig. 6), which are similar to those in the fluvial and lacustrine sediments near the
503 Taklamakan and Badanjilin Deserts and the aeolian sediments in the surrounding Gobi desert, but they are
504 slightly different from those in the Kumtag and Tenggeli Deserts (Zhang et al., 2020).

505 The analytical results from heavy mineral assemblages indicate that the provenance of sandy dunes in
506 the Hexi Corridor is mainly from "sands of in-situ rising" (Zhu et al., 1980; Chang, 2019). Researches from
507 palaeogeography believe that sediments from alluvial plains and alluvial deposits of ancient rivers,
508 lacustrine plain and lacustrine deposits of ancient lakes, aeolian deposits in the erosion zone of the
509 southern and northern foothills of the Hexi Corridor, and alluvial deposits of modern rivers are the main
510 material sources of sandy dunes in the Hexi Corridor (MDCES, 1975). Based on mineralogical analysis,
511 Ferrat et al. (2011) observed that sand dunes in the Hexi corridor have similar concentrations of mica,
512 quartz, illite, muscovite and albite with adjacent areas, such as the Tenggeli Desert and the Badanjilin
513 Desert. This similar mineralogical composition may lead to the similarity in geochemical characteristics of
514 aeolian sediments in these areas. Grain-size sedimentological and geochemical studies based on detrital
515 materials suggest that alluvial deposits in the Qilian Mountains, paleo-lacustrine deposits in low-level areas,
516 and surface aeolian deposits in Gobi desert areas are the main material sources for the formation and
517 development of sandy dunes in the Hexi Corridor (Wang and Wang, Zhang and Dong, 2015; Zhang et al.,
518 2016; Zhang et al., 2020).

519 Summarizing the above characteristics and evidences of sand dunes, it can be concluded that there
520 are two states of dunes in the Hexi Corridor in the past half century, that is, dynamic change and basically
521 stable. This kind of geomorphological evolution is closely related to its material source and regional



522 environmental conditions. Dried river deposits (playas), alluvial/proluvial deposits and lacustrine deposits
523 are the main sources of sandy dunes in the Hexi Corridor, while these detrital deposits mainly come from
524 the Qilian Mountains in the south and the Beishan Mountains in the north. Compared with sand dunes in
525 desert areas, sand dunes in the oasis area of the Hexi Corridor have more complex material sources. They
526 are closely linked to regional land degradation and desertification issues in the Hexi Corridor.

527

528 **4. 2. Mechanisms of land desertification in the Hexi Corridor**

529

530 Generally speaking, sandy dunes in the Hexi Corridor are dominated by the mobile dunes. In the early
531 research work, the formation of these mobile dunes was considered to be caused by the destruction of
532 vegetation previously fixed on the shrub dunes in the oasis; or because the gravel Gobi desert and related
533 wind-erosion areas in the Hexi Corridor provided abundant sandy sediments, resulting in a wide
534 aeolian-sand transportation and accumulation to form sandy dunes in the corridor area; or because that in
535 the arid Hexi Corridor, the shallow and intermittent rivers with broad riverbeds changed their courses and
536 the abandoned dried riverbeds were blown up by wind, causing accumulation of the fluvial sediments to
537 form sandy dunes near the river banks (Zhu et al., 1980). The mechanisms above-mentioned for the
538 formation of sandy dunes can explain the characteristics of the sporadic or sheet-like distribution of sandy
539 dunes in the Hexi Corridor, especially the characteristics of sandy dunes intermittently distributed along
540 the dried riverbeds by winding and zigzag patterns, and scattered on the gravel Gobi deserts at the edge of
541 oases.

542 Apart from the above natural causes, it is also believed that the formation of sandy dunes in the Hexi
543 Corridor is not all controlled by the influence of natural factors, some dunes should be formed in historical
544 periods and are the result of human activities (Zhu et al., 1980; Zhu and Chen, 1994; Zhu, 1999; Yang et al.,
545 2004; Chang et al., 2005; Li, 2007). For example, ruins of the Han, Tang, and Ming Dynasties and sites of
546 the Great Wall can also be found in some dune fields, such as the Shouchang ruins in the South Lake area
547 of Dunhuang, the ruins in the dune fields of the Xicheng Post Station to the west of Zhangye, and the sites
548 of the Great Wall of Ming Dynasty in the dune fields in the Minqin area (Zhu et al., 1980; Zhu and Chen,
549 1994; Zhu, 1999), etc.

550 Regarding the above desertification mechanisms, the wind-eroded fields in Gobi deserts and its
551 deflation products in the Western Hexi Corridor (the upper windward area) are considered to be one of the
552 reasons for the desertification of the middle and eastern Hexi Corridor, because the former may provide
553 the material basis for the latter to form sandy dunes. However, is the existence of these western Gobi and
554 wind erosion areas really the main cause of desertification in the Hexi Corridor?

555 In order to solve this problem, researches have been carried out on the Gobi soils, wind-erosion
556 landforms and the intensity and potential of the wind erosion process in the western Hexi Corridor (e.g.,



557 Zhu et al., 1980; Zhang et al., 2004; Qu et al., 2005; Wang et al., 2013; Yin et al., 2014, 2016; Zhang et al.,
558 2016; An et al., 2019; Hu et al., 2020). From the perspective of geomorphology, wind-eroded lands are
559 widely distributed in the western part of the Hexi Corridor. The result of surface wind erosion in these
560 areas is the formation of long strip-shaped aeolian monadnocks and deflation hollows (aeolian
561 depressions), which are roughly parallel to the wind direction. Generally, these wind-eroded landforms are
562 about 1~3 meters high, and a few are up to 5 meters (Zhu et al., 1980), which are roughly distributed
563 along the lower reaches of the Shule River and the western part of the Dunhuang Oasis. Studies on the
564 surface properties of gravel desert (Gobi) and its impact on wind erosion and dust emission in the west of
565 the Hexi Corridor have shown that the gravel Gobi is very different from the sandy desert (dune field)
566 because the grain-size composition of the surface sediment and the occurrence state (erodibility) of fine
567 granular material are completely different (Zhang et al., 2004; Yin et al., 2014, 2016; Zhang et al., 2016; Hu
568 et al., 2020). The surface of Gobi desert is composed of the gravel-, sand-, fine-sand- and clay-fraction
569 particles with coarse- and fine-grained materials mixed together, while the surface of dune field is mainly
570 composed of the medium-sand-fraction particles, with no or few coarser-grained gravels and finer-grained
571 silt and clay particles (Zhang et al., 2016; An et al., 2019). A salt crust usually exists on the surface of Gobi
572 desert in the west Hexi Corridor and thus the fine-grained particles are consolidated due to the presence
573 of salt cement, leading to a weak wind erodibility in Godi desert, while the surface of dunes is loose,
574 making a strong erodibility in dune field (Zhang et al., 2016). Because the potential sediment availability
575 (controlled by erodibility of surface fine-grained particles), the gravel coverage (surface roughness) and the
576 average particle size of surface sediments are the main factors affecting dust emission (Pye, 1987; Gillette
577 and Stockton, 1989; Raupach et al., 1993), the three factors will determine whether the Gobi desert in the
578 western Hexi corridor has potential contribution to regional desertification in the Hexi Corridor.

579 Based on field surveys and using the ImageJ software to process high-resolution image data, Zhang et
580 al. (2016) estimated the gravel coverage and surface salt crust status in different Gobi areas in the west
581 Hexi Corridor, determined the proportion of total surface sediment weight occupied by gravels (diameter >
582 2 mm), and analyzed the sedimentological grain-size distribution of different land surface sediments. The
583 results of this work show that: (1) in the west Hexi Corridor, the gravel coverage of Gobi surface is
584 moderate, with the gravel coverage mainly between 40% and 70% (average 52%, SD = ± 17%) (Zhang et al.,
585 2016). The rate of gravel coverage in this level can produce the maximum aerodynamic roughness on the
586 ground surface to prevent dust emission (Lyles and Tatarko, 1988; Wolfe and Nickling, 1996; Dong et al.,
587 2002a, 2002b; Liu and Dong, 2003; Uno et al., 2006; Rostagno and Degorgue, 2011). (2) Most of the Gobi
588 surface lands (75% of the total area) have formed salt crust. Only the areas with high sand-transport
589 potential of wind in the northern Hexi Corridor and the edge of sandy deserts have no surface salt crust. (3)
590 The content of erodible materials (sand, silt and clay) on the Gobi surface has a clear spatial distribution.



591 Sediments of the Gobi surface are mostly the medium-sand and fine-sand particles (52.5% and 25.0%,
592 respectively), while the silt and clay contents range from 9.8% to 40.1%, with most areas (about 73%)
593 ranging from 10% to 30%. (4) In most Gobi regions, the potential transport of sand material is > 200 vector
594 units, but 75% of these areas have solid soil crust on the ground surface (Zhang et al., 2016).

595 Combined the above indexes, i.e. the proportion of fine-grained dust materials, the coverage rate of
596 salt crust, and the potential transport of sand material, it is shown that the high level of gravel coverage
597 and surface crust rate in the west Heixi Corridor can effectively reduce the dust emission from the Gobi
598 surface. Therefore, the Gobi area in the west Heixi Corridor is not the main source area of sandstorms
599 occurred in the middle and east of the Hexi Corridor. The northern part of the Hexi Corridor may be the
600 main source area of dust.

601 Another potential indicator that can indicate the degree of modern desertification in the region
602 comes from the meteorological parameter, such as the number of sandstorm days and strong wind days
603 (Chang et al., 2019). Sandstorm refers to a windy and sandy weather phenomenon with the wind speed
604 \geq the sand-blowing wind speed and the horizontal visibility < 1,000 m. The Hexi Corridor is considered to
605 be one of the areas with the most-frequent (heavy) sandstorm in northwest China (Zhu et al., 1994; Zhu,
606 1999). The results of meteorological data analysis from the Hexi Corridor show that since 1956, the
607 number of local sandstorm days in the Hexi Corridor is about 11.20 day/year (Table 4), and the average
608 number of strong wind days (wind speed >8 grade/day) is about 18.39 days/year (Table 4), but the number
609 of local sandstorm days in the Hexi Corridor has shown a generally-decreasing trend (Fig. 7a), with a
610 decline rate of 0.677 times/year (Chang et al., 2011). In addition, the frequency of sandstorms throughout
611 northern China is also decreasing during the same period (Zhang and Ren, 2003; Li and Zhang, 2007).
612 However, this is contrary to the situation of global sandstorms, because the number of times of global
613 sandstorms is increasing in recent decades (Houghton et al., 2001; Ding, 2002). This indicates that the
614 sandstorm process in the Hexi Corridor and even in the entire northern China does not respond to the
615 global changes, revealing that the cause of desertification in the Hexi Corridor is different from other parts
616 of the world.

617 As shown in Fig. 7a, the number of sandstorm days in the Minqin area of the Hexi Corridor has shown
618 a decreasing trend as a whole since 1956-2008, and there are three sub-trends during this period, i.e.,
619 both the frequency and number of sandstorms decreased rapidly (1956-1969), the frequency was high and
620 stable (1971-1987), and the frequency was low and slowly decreased (1987-2008).

621 However, with global warming, the temperatures in desert areas are generally increasing (Fig. 7b),
622 and the frequency of sandstorms should have increased, but why has the actual situation reduced?

623 To answer this question, we need to analyze the climate change in arid northern China and the Hexi
624 Corridor since this period. For nearly half a century, global warming has become a worldwide concern. In



625 this context, how does the climate change and respond to global warming in the desert areas of northern
626 China and the Hexi corridor?

627 Researches on this issue have been carried out in arid regions of northern China and the Hexi Corridor
628 (e.g. Ding, 2002; Sha et al., 2002; Chang et al., 2011, 2016b). Here, we briefly summarize the research
629 results of climate change in the Hexi Corridor (the Minqin arean) in recent decades.

630 (1) From 1961 to 2008, the rising rate of the annual average temperature in the Minqin area was
631 higher than that of global temperature in the 20th century and that of China in the past 100 years. Among
632 them, the temperature increase in February was the largest, with the monthly average temperature
633 increasing by 3.01 °C (Fig. 7b).

634 (2) From the 1980s to 1990s, the warmest in the world in the 20th century, the extreme maximum
635 temperature in Minqin has increased significantly, while the extreme minimum temperature has decreased
636 intermittently, and the instability of the extreme maximum and minimum temperatures has increased. The
637 detailed results are as follows: the instability of the monthly average temperature in January and April
638 increases; the isothermal date in February is 10.36 days earlier; the instability of the extreme maximum
639 temperature in December and January increases; the variation coefficient of the extreme minimum
640 temperature in May is as high as 287% (Fig. 7C).

641 (3) During the period 1961-2008, the temperature in the Minqin area increased, the precipitation also
642 shown an increasing trend, and the air humidity also increased significantly (Fig. 7d, 7f).

643 (4) In the Minqin area, the instability of precipitation increased in January and the stability of annual
644 precipitation increased (Fig. 7e). In general, as with the large-scale regional climate change in northern
645 China, the problem of temperature instability should be more worthy of attention than the problem of
646 temperature warming (Ding, 2002; Sha et al., 2002; Chang et al., 2011, 2016b).

647 (5) The wind speed in the Minqin area continued to decrease during the period from 1961 to 2008,
648 (Fig. 7g).

649 (6) There is a significant negative correlation between the annual and seasonal distributions of
650 sandstorms and the relative humidity of air (Fig. 7h).

651 It can be seen from the above that although the temperature in the Hexi Corridor has increased (in
652 response to global warming), the precipitation has increased (in response to the enhancement of the Asian
653 Summer Monsoon climate), the relative humidity of the air has increased and the wind speed has
654 decreased. As a result of this environmental change, on the one hand, the dynamic force of dust-release
655 process will be reduced (because of the decrease in wind speed), and on the other hand, the viscosity of
656 the surface sediment particles will increase (because of the increase in humidity), which will reduce the
657 frequency of dust storm events. Therefore, since 1961, the decreasing trend of sandstorm days in the Hexi
658 Corridor is mainly due to the increase in the relative humidity of the air, that is, the warming and



659 humidification of the local climate is one of the main reasons responsible for the reduction of sandstorms
660 in the Hexi Corridor. In other words, the Hexi Corridor has a potential trend of reverse desertification in the
661 past half century. The main influencing factor of desertification in the Hexi Corridor is climate change, that
662 is, controlled by natural factors.

663

664 **4. 3. Environmental implications of land desertification in the Hexi Corridor**

665

666 For more than half a century, in response to the problem of desertification in the Hexi Corridor, local
667 governments and organizations have carried out systematic engineering and theoretical researches on
668 desertification control in the Hexi Corridor. The most significant works and researches have been done on
669 the ecological and geomorphological control of desertification, such as the study on the water physiology
670 and ecology of desert xerophytes, the study of desert climate change and its response to global warming,
671 the study of the phenology of desert plants, and the study of aeolian sediments accumulation on the edge
672 of oasis, etc (Zhu and Wang, 1994; Zhu, 1999). These ecological studies also highlight that the ecological
673 and water environment of the Hexi Corridor has changed greatly with the above-mentioned climatic and
674 geomorphological changes in the Hexi Corridor, such as:

675 (1) The groundwater level in the Hexi Corridor has fallen and the regional water resources have
676 decreased. For example, the 26 motorized wells located in the inner Minqin Oasis indicate that the
677 groundwater level in the central part of the Minqin Oasis fell at a rate of 0.54m/y during the period
678 1985-2001 (Fig. 8); and the 7 motorized wells located at the edge of the Minqin Oasis indicates that the
679 groundwater level in the marginal area of the Minqin Oasis also decreased, with a drop rate of 0.56m/y
680 from 1985 to 2017 (Fig. 8).

681 (2) The area of natural sand-fixing forests in the Hexi Corridor has decreased. Due to the drop of
682 groundwater level, the natural sand-fixing vegetation in the Minqin area has declined on a large scale, and
683 the desert steppe has become sandy field. For example, in 1981, the area of natural sand-fixing forest in
684 the Minqin area was 203,951 hm², but by 2002, the area of natural sand-fix forest had decreased to
685 197,353 hm² (Table 5); in the early 1980s, there were 373 hm² of *Populus euphratica* forest in Minqin, but
686 it has now disappeared (Table 5).

687 The above ecological and hydrological problems tell us that in an arid and desertified environment
688 such as the Hexi Corridor, the reason for the continuous decrease of vegetation is not the lack of
689 afforestation, nor the change of regional precipitation or relative humidity (although the climate in the
690 Hexi Corridor has become more humid in the past half century, as illustrated in Fig. 7), but is subject to the
691 changes of "effective water", such as groundwater and soil water (Fig. 8). In other words, effective
692 moisture is the most restrictive factor for ecological sustainability in the desert environment. Therefore,
693 the control of desertification in an arid environment should be based on the principle of "centering on



694 effective water balance". Deviating from the principle of "effective water balance" is a deviation from the
695 basic law of natural environment change in sandy areas. In this contradiction, it is difficult to achieve the
696 control of desertification without the overall direction of water-saving management and research on
697 groundwater.

698 Therefore, it can be said that the change of water environment is one of the leading factors restricting
699 the change of the ecological environment from an oasis landscape toward a desertified landscape in arid
700 areas. The degradation of the ecological environment in the lower reaches of the Shiyang River Basin in the
701 Hexi Corridor, once again illustrates this point. From a larger spatial scale, the arid and semi-arid areas in
702 northern China are seriously deficient in water resources. How to combat desertification is the primary
703 problem restricting the sustainable development of the region. Some scholars believe that the transfer of
704 water from the outer basins (such as the Yellow River Basin and the Yangtze River Basin) can appropriately
705 alleviate the serious water shortage and desertification in the inland area of the Hexi Corridor. However, is
706 such a measure feasible? In view of the large-scale allocation of resources in arid areas, on the one hand,
707 the transfer of water from the outer basin is not the fundamental solution to the problem, and it is likely to
708 cause ecological problems in other watersheds, because almost every watershed under arid environment
709 is short of water or potentially short of water. On the other hand, large-scale water transfer is also
710 unrealistic. Due to the constraints of socio-economic conditions and financial resources in the Hexi
711 Corridor, it is not feasible to transfer water from the outer basin at least in the near future. We believe that
712 the fundamental way to solve the problem of water resources of the inland areas of the Hexi Corridor lies
713 in the rational utilization of existing water resources. Furthermore, some studies believe that the inland
714 areas of the Hexi Corridor are not an absolute "resource-based water shortage", but a combination of
715 "resource-based water shortage" and "technics-based water shortage" coexist (Chang and Liu, 2003). It
716 means that the utilization of water resources is unreasonable and the efficiency of utilization is not high.
717 Comprehensive control is the only way to combat desertification in the interior of the Hexi Corridor.

718

719 5. Conclusion

720

721 The formation and dynamic change of sandy dune landforms in the Hexi Corridor is a typical problem
722 of land desertification in the mid-latitudes of Northern Hemisphere, which has attracted great attention
723 from China and the international community for nearly half a century. It is of great significance to study the
724 formation and evolution of aeolian dunes in this area to reveal the process and mechanism of
725 desertification and the related environmental changes. Based on the existing high-resolution satellite
726 image interpretations, field investigations and observations, comprehensive understanding of the
727 evidences from geomorphological, aeolian-physical, granulometrical and geochemical analysis, this study
728 discussed the formation of dune landform, the mechanism of desertification and their environmental



729 implications in the Hexi Corridor. The analytical results show that 80% of the sand particles flow within a
730 height of 20~30 cm near the surface, and about half of the sand particles flow within a height of 0.3~0.5
731 cm near the surface in the Hexi Corridor. The average height of the typical crescent-shaped dunes is about
732 6.75m, and the minimum and maximum values are between 2.6 and 11.2m. In terms of the inter-annual
733 and multi-year dynamic characteristics of the sandy dunes in the Hexi Corridor, only the crescent-shaped
734 dunes and chains of barchan dunes are moving or wigwagging, while the parabolic and longitudinal dunes
735 did not move. Under the influence of wind speed, strong wind days and other factors, the dunes at the
736 edge of the Minqin Oasis move the fastest, with a moving speed of about 6.2m/a. Affected by the main
737 wind direction and other factors, the dunes at the edge of the Dunhuang Oasis move the slowest, with a
738 moving speed of about 0.8m/a. The main factors affecting the dynamic changes of sandy dunes in the Hexi
739 Corridor are the annual precipitation, the annual average wind speed and the number of annual strong
740 wind days, of which the annual precipitation contributes the largest, indicating that the climate factors
741 have a most important impact on the dynamic change of sand dunes. The cumulative curve of particle size
742 frequency of dune sediments in the Hexi Corridor basically presents a three-segment model, indicating
743 that the dune sediments are mainly in a saltation mode under the action of wind force, superimposed with
744 a small amount of coarser and finer particles dominated by the creeping and suspension models, which is
745 obviously different from that of the Gobi sediments with a dominant two-segment model. The early and
746 recent investigations of dune sources and the sedimentological and geochemical evidences indicate that
747 the sandy dunes in the Hexi Corridor are mainly derived from "locally or in-situ raised sediments", which
748 are mainly come from alluvial plains and ancient fluvial sediments, as well as ancient lake plains and
749 lacustrine deposits in the Hexi Corridor, aeolian deposits in the piedmont denudation zones of the north
750 and south mountains and modern fluvial sediments. In terms of the abundance of major and trace
751 elements, the crescent-shaped dunes in the Hexi Corridor have certain similarities and differences to other
752 sandy dunes in the northwest and northern deserts of China (such as the Kumtag, Badanjilin, Tenggeli, and
753 Taklamakan Deserts, etc.) or aeolian loess in the Loess Plateau. The sandy dunes in the Hexi Corridor are
754 relatively rich in iron and Co. Considering the proportion of fine particles on the surface, the coverage rate
755 of surface salt crust, and the potential migration of erodible sandy materials, it can be concluded that the
756 Gobi in the west of the Hexi Corridor is not the main source area of sandstorms in the middle and east of
757 the corridor, but the north is probably the main source area of dust. In the past half century, the warming
758 and humidification of the local climate is one of the main causes of the reduction of sandstorms in the
759 study area. During the same period, the Hexi Corridor has a potential trend of anti-desertification, which is
760 mainly controlled by climate change, that is, an influence of natural factors. But in the oasis area of the
761 Hexi Corridor, the effective measures to restrict desertification depend on human activities.
762 Comprehensive management and rational utilization of the existing water resources, especially the
763 restriction of the decline of groundwater, is the key to preventing desertification in oases, rather than



764 water transfer from outer river basins.

765

766 **Acknowledgments**

767

768 The study was financially supported by the National Natural Science Foundation of China (grant nos.
769 41930640, 41771014) and the Project of the Second Comprehensive Scientific Investigation on the Qinghai
770 Tibet Plateau (2019QZKK1003). Sincere thanks are extended to Profs. Xiaoping Yang, Zhaofeng Chang,
771 Zhibao Dong and Zhengcai Zhang for their help in the author's (BZ) research work.

772

773 **References**

774

- 775 An F, Zhang D, Zhao J, Chai C, Zhao Y, Sun T. Physical and chemical properties of soils in different types in
776 the Gobi areas of the Hexi Corridor. 2019, 6, 42-47 (in Chinese with English abstract).
- 777 Bagnold R A. Physics of sand and dunes in desert. Beijing: Science Press. 1959.
- 778 Chang Z, Liu H. Desertification control in Hexi inland river basins of Gansu Province (II). Protection Forest
779 Science and Technology, 2003, 2, 28-32 (In Chinese with English Abstract).
- 780 Chang Z, Zhao M, Han F, Zhong S, Liang T. Natural and artificial factors and their transfer on sandy
781 desertification of lower reaches of Shiyang River Basin. Arid Land Geography, 2005, 28(2), 150-155 (in
782 Chinese with English abstract).
- 783 Chang Z, Han F, Zhong S. Response of desert climate change to global warming in Minqin, China. Journal of
784 Desert Research, 2011, 31(2), 505-510 (In Chinese with English Abstract).
- 785 Chang Z, Wang Q, Zhang J, Xi J, Wang Q, Zhang D, Tang J, Zhang H. Environmental conditions of barchans
786 dune and barchans chain – a case study from the Hexi Desert area of Gansu. Animal Husbandry
787 and Feed Science, 2015, 7(6), 383-388.
- 788 Chang Z, Zhu S, Shi X, Zhang J, Li Y, Wang Q, Zhang D, Duan X. Comparisons between movement speed of
789 main types of dunes: a case study of desert areas in Hexi region of Gansu Province. Journal of
790 Landscape Research, 2016a, 8(6), 36-40.
- 791 Chang Z, Ma Z, Wang D, Han F, Duan X, Wang Q, Zhang J. Instability of climate change in the Minqin Desert
792 Area. Arid Zone Research, 2016b, 33(3), 601-608 (in Chinese with English Abstract).
- 793 Chang Z, Li Y, Zhang J, Wang Q, Zhang D, Tang J, Wang Q, Zhang H. Stability mechanisms of barchan sand
794 dunes: a case study in the Hexi Desert in Gansu. Acta Ecologica Sinica, 2017, 37(13), 4375-4383 (in
795 Chinese with English abstract).
- 796 Chang Z. Problems and solutions to desertification combating in the Hexi, Gansu for 60 years. Journal of
797 Arid Land Resources and Environment, 2019, 33(9), 152-159 (in Chinese with English Abstract).
- 798 Chen F, Liu Y. Secular annual movement of sand dunes in Badain Jaran Desert based on geographic



- 799 analyses of remotely sensed imagery. *Remote Sensing Technology and Application*, 2011, 26(4),
800 501-507.
- 801 Chen F, Zhang J, Liu J, Cao X, Hou J, Zhu L, Xu X, Liu X, Wang M, Wu D, Huang L, Zeng T, Zhang S, Huang W,
802 Zhang X, Yang K. Climate change, vegetation history, and landscape responses on the Tibetan Plateau
803 during the Holocene: a comprehensive review. *Quaternary Science Reviews*, 2020, 243, 106444, doi:
804 10.1016/j.quascirev.2020.106444.
- 805 Ding Y. Global climate change. *World Environment*, 2002, 6, 9-12.
- 806 Ding Y. Prediction of environmental changes in Western China. In: Qin D (editor), *Assessment of*
807 *Environmental Evolution in Western China*. Science Press, Beijing, 2002. pp. 1-231.
- 808 Dong Y, Huang D. Preliminary observation of movement of coastal dunes in Feicui Island in Changli, Hebei
809 Province. *Journal of Desert Research*, 2013, 33(2), 486-492.
- 810 Dong Z, Chen G, Yan C, Han Z, Wang X. Movement laws of dunes along oiltransportation highway in the
811 Tarim Desert. *Journal of Desert Research*, 1998, 18(4), 328-333 (in Chinese with English abstract).
- 812 Dong Z, Qu J, Liu X, Zhang W, Wang X. Experimental investigation of the drag coefficients of gobi surfaces.
813 *Science in China Series D - Earth Sciences*, 2002a, 45(7), 609–615.
- 814 Dong Z, Liu X, Wang X. Aerodynamic roughness of gravel beds. *Geomorphology*, 2002b, 43(1-2), 17-31.
- 815 Dong Z, Su Z, Qian G. *Aeolian landforms in the Kumtag Desert*. Science Press, Beijing. 2011.
- 816 Ferrat M, Weiss DJ, Strekopytov S, Dong SF, Chen HY, Najorka J, Sun YB, Gupta S, Tada R, Sinha R. Improved
817 provenance tracing of Asian dust sources using rare earth elements and selected trace elements for
818 palaeomonsoon studies on the eastern Tibetan Plateau. *Geochimic & Cosmochimic Acta*, 2011, 75,
819 6374–6399.
- 820 Finkel H J. The barchans southern peru. *The Journal of Geology*, 1959, 67(6), 628-631.
- 821 Gillette DA, Stockton PH. The effect of nonerodible particles on wind erosion of erodible surfaces. *Journal*
822 *of Geophysical Research*, 1989, 94(12), 885-893.
- 823 Goudie A. *Great Warm Deserts of the World: Landscapes and Evolution*. Oxford University Press, New York,
824 2002.
- 825 Guo Z, Ruddiman W, Hao Q, Wu H, Qiao Y, Zhu R, Peng S, Wei J, Yuan B, Liu T. Onset of Asian desertification
826 by 22 Myr ago inferred from loess deposits in China. *Nature*, 2002, 416, 159-163.
- 827 Guo Z, Peng S, Hao Q, Biscaye P, An Z, Liu T. Late Miocene-Pliocene development of Asian aridification as
828 recorded in the Red-earth Formation in northern China. *Global and Planetary Change*, 2004, 41,
829 135-145.
- 830 He J, Guo J, Xing E, Cui W, Li J. Structure of wind-sand flow and movement laws of dunes along the Yellow
831 River in Ulan Buh Desert. *Transactions of the Chinese Society of Agricultural Engineering*, 2012, 28(17),
832 71-77 (in Chinese with English abstract).
- 833 Honda M, Shimizu H. Geochemical, mineralogical and sedimentological studies on the Taklimakan Desert



- 834 sands. *Sedimentology*, 1998, 45, 1125–1143.
- 835 Houghton JT, Ding Y, Griggs DJ, Noguier M, van der Linden PJ, Dai X, Maskell K, Johnson CA. *Climate Change*
836 2001: The scientific Basis. Cambridge University Press, Cambridge, UK, 2001. pp15-108.
- 837 Hu F, Zhang K, An Z, Yu Y. Composition of wind dynamic environment among desert, oasis and gobi. *Journal*
838 of Desert Research, 2020, 40(4), 113-119 (in Chinese with English abstract).
- 839 Hu X, Wang M, Liu Y. Analysis of movement of dunes in the Tengger Desert based on high-resolution
840 remote sensing images. *China Science and Technology Review*, 2016, 2, 337.
- 841 Jiang Q, Yang X. Sedimentological and geochemical composition of aeolian sediments in the Taklamakan
842 Desert: Implications for provenance and sediment supply mechanisms. *Journal of Geophysical*
843 *Research Earth Surface*, 2019, 124, 1217–1237.
- 844 Lancaster N, Yang X, Thomas D. Spatial and temporal complexity in Quaternary desert datasets:
845 Implications for interpreting past dryland dynamics and understanding potential future changes.
846 *Quaternary Science Reviews*, 2013, 78, 301-302.
- 847 Lancaster N, Wolfe S, Thomas D, Bristow C, Bubenzer O, Burrough S, Duller G, Halfen A, Hesse P, Roskin J,
848 Singhvi A, Tsoar H, Tripaldi A, Yang X, Zarate M. The INQUA Dunes Atlas chronologic database.
849 *Quaternary International*, 2016, 410, 3-10.
- 850 Lang L, Wang X, Zhu B, Wang X, Hua T, Wang G, Li H, Zhang C. Nebkha formation and variations in sediment
851 availability and wind-energy regime of the western Hexi Corridor over the past several decades.
852 *Journal of Desert Research*, 2017, 37(4), 611-620 (in Chinese with English abstract).
- 853 Li B. The oasis in the lower reaches of the Shiyang River has become the "the second Loulan" before the
854 mid-Tang Dynasty . *Research and Development*, 2007, 2, 153-157 (in Chinese).
- 855 Li E. Comparative Study on Characteristics of Aeolian Sediments between the Badanjinlin and Tengeli
856 deserts. Ph.D doctoral dissertation, Shaanxi Normal University, Xi'an, 2011 (in Chinese with English
857 abstract).
- 858 Li Y, Zhang S. Review of the Research on the relationship between sand-dust storm and arid in China.
859 *Advances in Earth Science*, 2007, 22(11), 1169-1176 (in Chinese with English abstract).
- 860 Liu T. *Loess and the Environment*. China Ocean Press, Beijing, 1985 (in Chinese).
- 861 Liu X, Dong Z. Aerodynamic roughness of gravel bed. *Journal of Desert Research*, 2003, 23(1), 40-47 (in
862 Chinese).
- 863 Lyles L, Tatarko J. Soil wind erodibility index in seven northern central states. *Transactions of the ASAE*,
864 1988, 31(5), 1396-1399.
- 865 Mao D, Lei J, Zhou J, Xue J, wang C, Rehemutula Z. Movement rules of different shifting dunes and
866 semi-shifting dunes in Cele, Xinjiang Uygur Autonomous Region. *Research of Soil and Water*
867 *Conservation*, 2016, 23(3), 278-282.
- 868 MDCES (Minqin Desert Control Experiment Station). *Deserts and Control in Gansu*. Lanzhou: Gansu



- 869 People's Publishing house, 1975. Pp.33-38.
- 870 Muhs D. Mineralogical maturity in dunefields of North America, Africa and Australia. *Geomorphology*, 2004,
871 59, 247–269.
- 872 Muhs D, Bush C, Cowherd S, Mahan S. Geomorphic and geochemical evidence for the source of sand in the
873 Algodones dunes, Colorado Desert, southeastern California. In: Tchakerian V (Ed), *Desert Aeolian*
874 *Processes*. Chapman & Hall, London, 1995. pp. 37–74.
- 875 Muhs D, Stafford T, Cowherd S, Mahan S, Kihl R, Maat P, Bush C, Nehring J. Origin of the Late Quaternary
876 dune fields of northeastern Colorado. *Geomorphology*, 1996, 17, 129–149.
- 877 Pan K, Zhang Z, Dong Z, Zhang C, Li X. Physicochemical characteristics of surface sediments of
878 crescent-shaped sand dunes in the Hexi Corridor, Gansu, China. *Journal of Desert Research*, 2019,
879 39(1), 44-51 (in Chinese with English abstract).
- 880 Pease P, Tchakerian V, Tindale N. Aerosols over the Arabian Sea: geochemistry and source areas for aeolian
881 desert dust. *Journal of Arid Environments*, 1998, 39, 477–496.
- 882 Pease P, Tchakerian V. Geochemistry of sediments from Quaternary sand ramps in the southeastern
883 Mojave Desert, California. *Quaternary International*, 2003, 104, 19–29.
- 884 Pettijohn FJ, Potter PE, Siever R. *Sand and Sandstone*. Springer-Verlag, New York, 1972.
- 885 Pu Z. For the lost oasis - a review of studies on desertification in the Hexi Corridor during the historical
886 period. *Collections of Essays On Chinese Historical Geography*, 2005, 20 (1), 157-158 (in Chinese).
- 887 Pye K. *Aeolian Dust and Dust Storms*. Academic Press, Gainesville, 1987.
- 888 Qu J, Huang N, Ta W, Lei J, Dong Z. Structural characteristics of Gobi sanddrift and its significance. *Advances*
889 *in Earth Science*, 2005, 20(1), 19-23 (in Chinese with English abstract).
- 890 Raupach MR, Gillette DA, Leys JF. The effect of roughness elements on wind erosion threshold. *Journal of*
891 *Geophysical Research*, 1993, 98(D2), 3023-3029.
- 892 Ren X. Element analysis of surface sediments from active dunes in the Minqin Oasis and its adjacent
893 deserts. Ma.D Dissertation, Lanzhou University, Lanzhou, 2010 (in Chinese with English abstract).
- 894 Ren X, Liu T, Wang Z. Characters of geomorphologic parameter about barchans dunes. *Research of Soil and*
895 *Water Conservation*, 2010, 17(1), 163-166 (in Chinese with English abstract).
- 896 Ren X, Wang Z. The provenance of eolian sediments in Minqin Oasis, Gansu Province. *Journal of Ningxia*
897 *University Natural Science Edition*, 2010, 31(1), 88-92 (in Chinese with English abstract).
- 898 Ren X, Yang X, Wang Z, Zhu B, Zhang D, Rioual P. Geochemical evidence of the sources of aeolian sands and
899 their transport pathways in the Minqin Oasis, northwestern China. *Quaternary International*, 2014,
900 334-335, 165-178.
- 901 Rostagno CM, Degorgue G. Desert pavements as indicators of soil erosion on aridic soils in north-east
902 Patagonia (Argentina). *Geomorphology*, 2011, 134, 224-231.
- 903 Sahu BK. Depositional mechanisms from the size analysis of clastic sediments. *Journal of Sedimentary*



- 904 Research, 1964, 34(1), 73–83.
- 905 Sha W, Shao X, Huang M. Climate warming and its impact on natural regional boundaries in China since
906 1980s. *Science China in Series D*, 2002, 32 (4), 317-326.
- 907 Shi X, Li G, Liu S, Wei Y. Dynamic changes of barchans dunes and its relationship with meteorological
908 factors along oasis fringe in Hexi Corridor. *Journal of Gansu Agricultural University*, 2018, 2, 86-93 (In
909 Chinese with English Abstract).
- 910 Sun J. Provenance of loess material and formation of loess deposits on the Chinese Loess Plateau. *Earth
911 and Planetary Science Letters*, 2002, 203, 845e859.
- 912 Taylor, S.R., McLennan, S.M., 1985. *The Continental Crust: Its Composition and Evolution*. Blackwell
913 Scientific Publications, London.
- 914 Uno I, Wang Z, Chiba M, Chun Y, Song S, Hara Y, Jung E, Lee SS, Liu M, Mikami M, Music S, Nickovic S,
915 Satake S, Shao Y, Song Z, Sugimoto N, Tanaka T, Westphal DL. Dust model intercomparison (DMIP)
916 study over Asia: overview. *Journal of Geophysical Research*, 2006, 111, D12213, doi:
917 10.1029/2006JD006575.
- 918 Visher G. Grain size distributions and depositional processes. *Journal of Sedimentary Research*, 1969, 39(3),
919 1074-1106.
- 920 Wang J, Liu L, Shen L. Research of movement laws of barchan dunes in the Mu Us sandy land based on
921 Google Earth software. *Remote Sensing Technology and Application*, 2013, 28(6), 1094-1100.
- 922 Wang L. Surface deposits in the Hexi Corridor and its adjacent areas and implications for provenance of
923 Asian dust. Ma.D Dissertation, Lanzhou University, Lanzhou, 2011 (in Chinese with English abstract).
- 924 Wang L, Wang Q. Elemental compositions of surface deposits in the Hexi Corridor and its adjacent areas,
925 northwestern China. *Northwestern Geology*, 2013, 46(2), 69-80 (in Chinese with English abstract).
- 926 Wang T. *Desert and Desertification in China*. Hebei Science and Technology Press, Shijiazhuang, 2003 (in
927 Chinese).
- 928 Wang X, Lang L, Hua T, Zhang C, Wang Z. Gravel cover of Gobi desert and its significance for wind erosion:
929 an experimental study. *Journal of Desert Research*, 2013, 33(2), 313-319 (in Chinese with English
930 abstract).
- 931 Wang X, Hua T, Zhu B, Lang L, Zhang C. Geochemical characteristics of the fine-grained component of
932 surficial deposits from dust source areas in northwestern China. *Aeolian Research*, 2018, 34, 18-26.
- 933 Williams M. *Climate Change in Deserts: Past, Present and Future*. Cambridge University Press, New York,
934 2014.
- 935 Wolfe SA, Nickling WG. Shear stress partition in sparsely vegetated desert canopies. *Earth Surface
936 Processes and Landforms*, 1996, 21, 607-619.
- 937 Wolfe S, Muhs D, David P, McGeehin J. Chronology and geochemistry of Late Holocene eolian deposits in



- 938 the Brandon Sand Hill, Manitoba, Canada. *Quaternary International*, 2000, 67, 61–74.
- 939 Yang X, Rost KT, Lehmkuhl F, Zhu Z, Dodson J. The evolution of dry lands in northern China and in the
940 Republic of Mongolia since the Last Glacial Maximum. *Quaternary International*, 2004, 118-119,
941 69-85.
- 942 Yang X. Desert research in northwestern China. A brief review. *Geomorphologie: Relief, Processus,*
943 *Environment*, 2006, 4, 275-284.
- 944 Yang X, Zhu B, White PD. Provenance of aeolian sediment in the Taklamakan Desert of western China,
945 inferred from REE and major-elemental data. *Quaternary International*, 2007, 175, 71-85.
- 946 Yang X, Scuderi L, Paillou P, Liu Z, Li H, Ren X. Quaternary environmental changes in the drylands of China e
947 a critical review. *Quaternary Science Reviews*, 2011, 30, 3219-3233.
- 948 Yang X, Li H, Conacher A. Large-scale controls on the development of sand seas in northern China.
949 *Quaternary International*, 2012, 250, 74-83.
- 950 Yin D, Qu J, Zu R, Tan L, An Z. Impact of disturbing on amount of wind erosion of sandy Gobi. *Journal of*
951 *Desert Research*, 2014, 34(1), 1-8 (in Chinese with English abstract).
- 952 Yang X, Liang P, Zhang D, Li H, Rioual P, Wang X, Xu B, Ma Z, Liu Q, Ren X, Hu F, He Y, Rao G, Chen N.
953 Holocene aeolian stratigraphic sequences in the eastern portion of the desert belt (sand seas and
954 sandy lands) in northern China and their palaeoenvironmental implications. *Science China Earth*
955 *Sciences*, 2019, 62, 1302-1315.
- 956 Zhang K, Qu J, Zu R, Fang H. Wind tunnel simulation about the effects of the different underlying surfaces
957 on the features of drifting sand current. *Arid Land Geography*, 2004, 37(3), 352-355 (in Chinese with
958 English abstract).
- 959 Zhang L, Ren G. Change in dust storm frequency and the climatic controls in northern China. *Acta*
960 *Meteorologica Sinica*, 2003, 61(6), 744-750 (in Chinese with English abstract).
- 961 Zhang Z, Dong Z. Dune field patterns and wind environments in the middle reaches of the Heihe Basin.
962 *Journal of Desert Research*, 2014, 34(2), 332-341 (in Chinese with English abstract).
- 963 Zhang Z, Dong Z. Grain size characteristics in the Hexi Corridor Desert. *Aeolian Research*, 2015, 18, 55-67.
- 964 Zhang Z, Dong Z, Li J, Qian G, Jiang C. Implications of surface properties for dust emission from gravel
965 deserts (gobis) in the Hexi Corridor. *Geoderma*, 2016, 268, 69-77.
- 966 Zhang Z, Dong Z, Zhang C, Qian G, Lei C. The geochemical characteristics of dust material and dust sources
967 identification in northwestern China. *Journal of Geochemical Exploration*, 2017, 175, 148-155.
- 968 Zhang Z, Pan K, Zhang C, Liang A. Geochemical characteristics and the provenance of aeolian material in
969 the Hexi Corridor Desert, China. *Catena*, 2020, 104483, doi: 10.1016/j.catena.2020.104483.
- 970 Zhu B. Geochemistry, hydrochemistry and sedimentology of the Taklamakan Desert in Tarim Basin, NW
971 China. Ph.D doctoral dissertation, Institute of Geology and Geophysics Chinese Academy of Sciences,
972 Beijing, 2007.



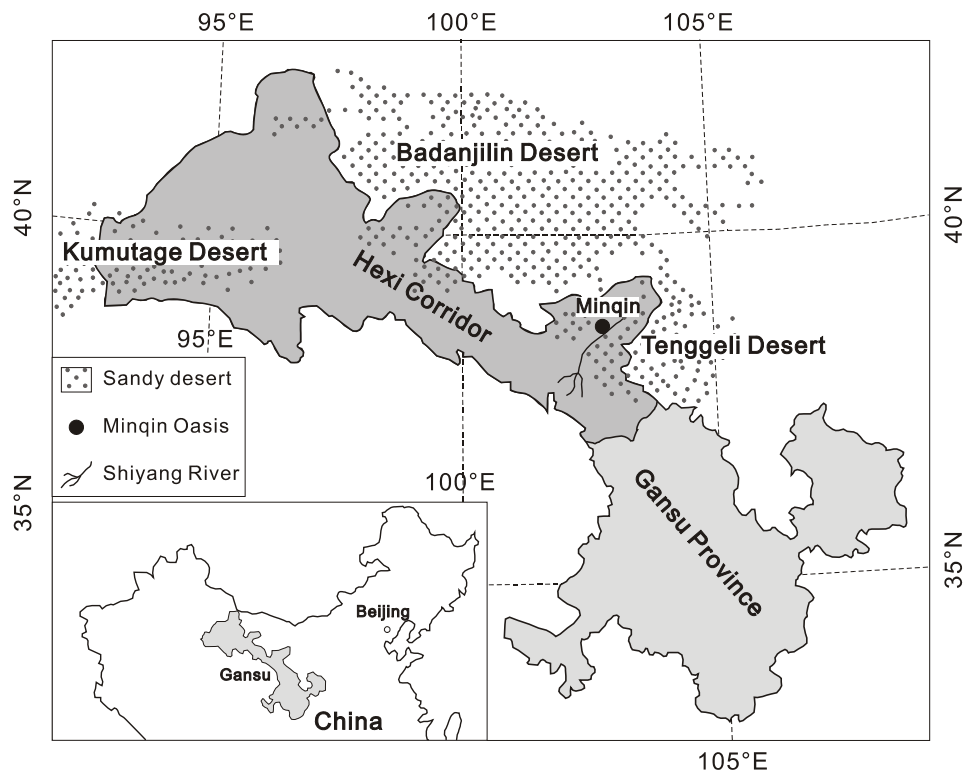
- 973 Zhu B, Yang X. Chemical Weathering of Detrital Sediments in the Taklamakan Desert, Northwestern China
974 Chemical Weathering of Detrital Sediments in the Taklamakan Desert, Northwestern China.
975 Geographical Research, 2009, 47(1), 57-70.
- 976 Zhu B, Yu J. Aeolian sorting processes in the Ejina desert basin (China) and their response to depositional
977 environment. Aeolian Research, 2014, 12, 111–120.
- 978 Zhu B, Yu J, Rioual P, Ren X. Particle size variation of aeolian dune deposits in the lower reaches of the
979 Heihe River basin, China. Sedimentary Geology, 2014, 301, 54–69.
- 980 Zhu Z, Guo H, Wu Q. Study on the movement of dunes near oases in the southwest of the Taklimakan
981 Desert. Acta Geographica Sinica, 1964, 30(1), 35-50.
- 982 Zhu Z, Wu Z, Liu S, Di, X. An Outline of Chinese Deserts. Science Press, Beijing, 1980 (in Chinese).
- 983 Zhu Z, Chen Z, Wu Z, Li J, Li B, Wu G. Study on the Geomorphology of Wind-drift Sands in the Taklamakan
984 Desert. Science Press, Beijing, 1981 (in Chinese).
- 985 Zhu Z, Wang T. Theory and practice on sandy desertification in China. Quaternary Sciences, 1992, 2, 97-106
986 (in Chinese with English abstract).
- 987 Zhu Z, Chen G. Sandy Desertification in China. Science press, Beijing, 1994 (in Chinese).
- 988 Zhu Z. Deserts, Desertification, Land Degradation and Strategies for Rehabilitation in China. Environmental
989 Press, Beijing, 1999 (in Chinese).
- 990 Zimbelman J, Williams S. Geochemical indicators of separate sources for eolian sands in the eastern
991 Mojave Desert, California, and western Arizona. Geological Society of America Bulletin, 2002, 114,
992 490–496.
- 993 Znamenski A И. Formation mechanisms of barchan dunes. Feodorovitch. Symposium of origin and research
994 methods of desert landscape. Science Press, Beijing, 1962. Pp. 104-109.
- 995
996
997



998
999
1000
1001

Figures and Figure Captions:

Fig. 1 Geographical position of the Hexi Corridor in China

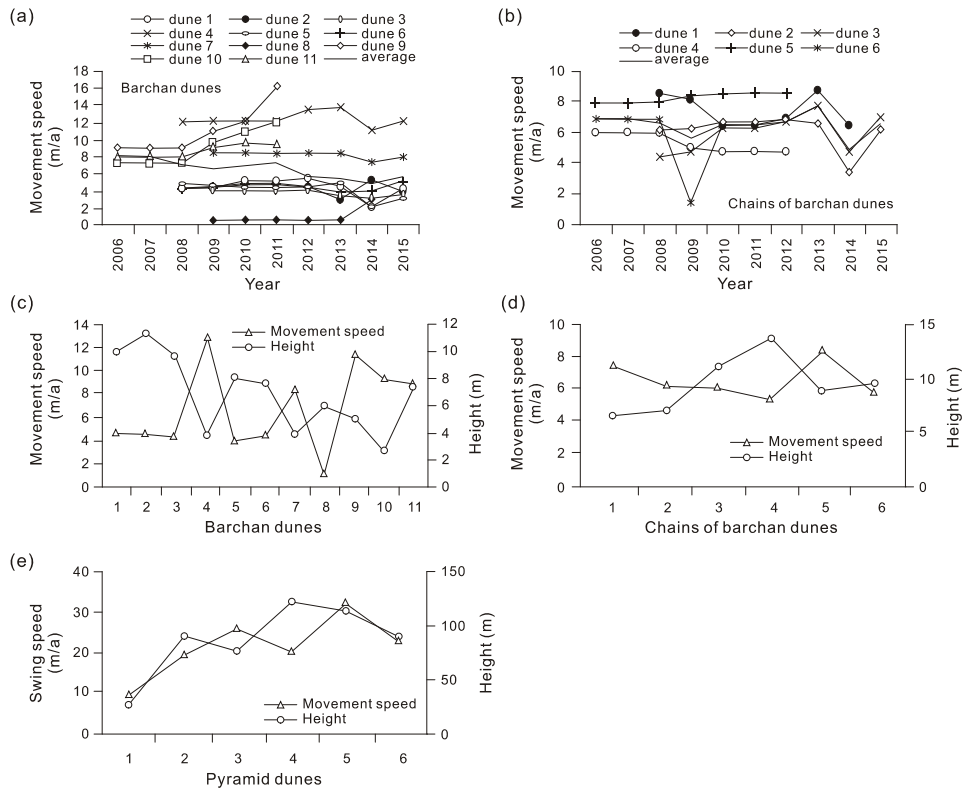


1002
1003
1004
1005
1006
1007
1008
1009
1010
1011
1012
1013
1014
1015
1016
1017
1018
1019
1020
1021
1022



1027
 1028
 1029
 1030
 1031
 1032
 1033
 1034
 1035

Fig. 3 The moving speed and height of sandy dunes in the Hexi Corridor (modified after Chang et al., 2016a). (a) the moving speed of crescent-shaped (barchan) dunes (see Table 1 for geographical locations of the corresponding dune IDs); (b) the moving speed of chains of barchan dunes (see Table 1 for geographical locations of the corresponding dune IDs); (c) the moving speed and height of barchans dunes (see Table 1 for geographical locations of the corresponding dune IDs); (d) the moving speed and height of chains of barchan dunes (see Table 1 for geographical locations of the corresponding dune IDs); (e) the movement speed and height of pyramidal dunes (see Table 1 for geographical locations of the corresponding dune IDs).

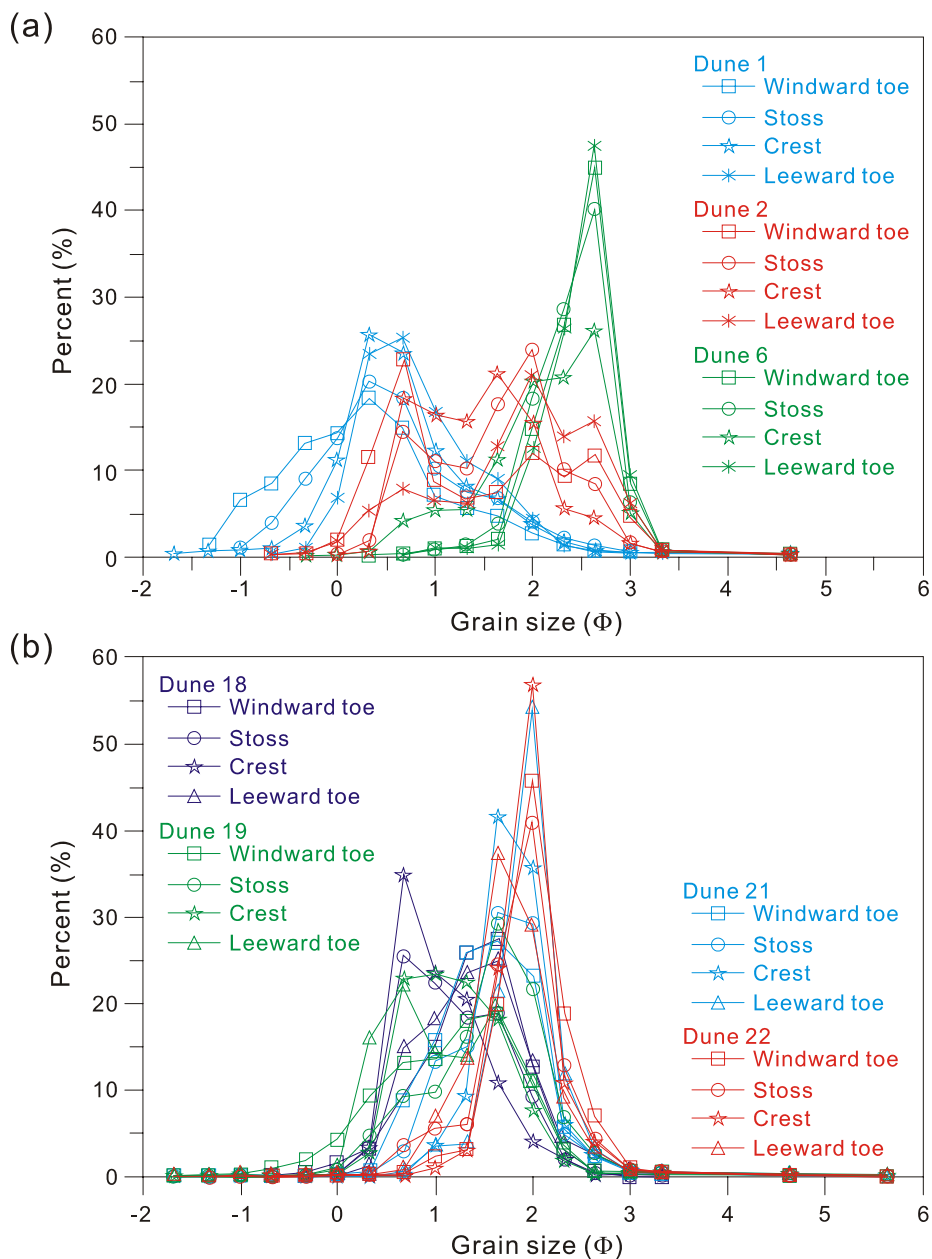


1036
 1037
 1038
 1039
 1040
 1041
 1042
 1043
 1044
 1045
 1046
 1047
 1048
 1049
 1050
 1051



1052
 1053
 1054

Fig. 4 The probability cumulative distribution curves of grain size of dune sediments in the Hexi Corridor (modified from Zhang and Dong, 2015)



1055
 1056
 1057
 1058
 1059

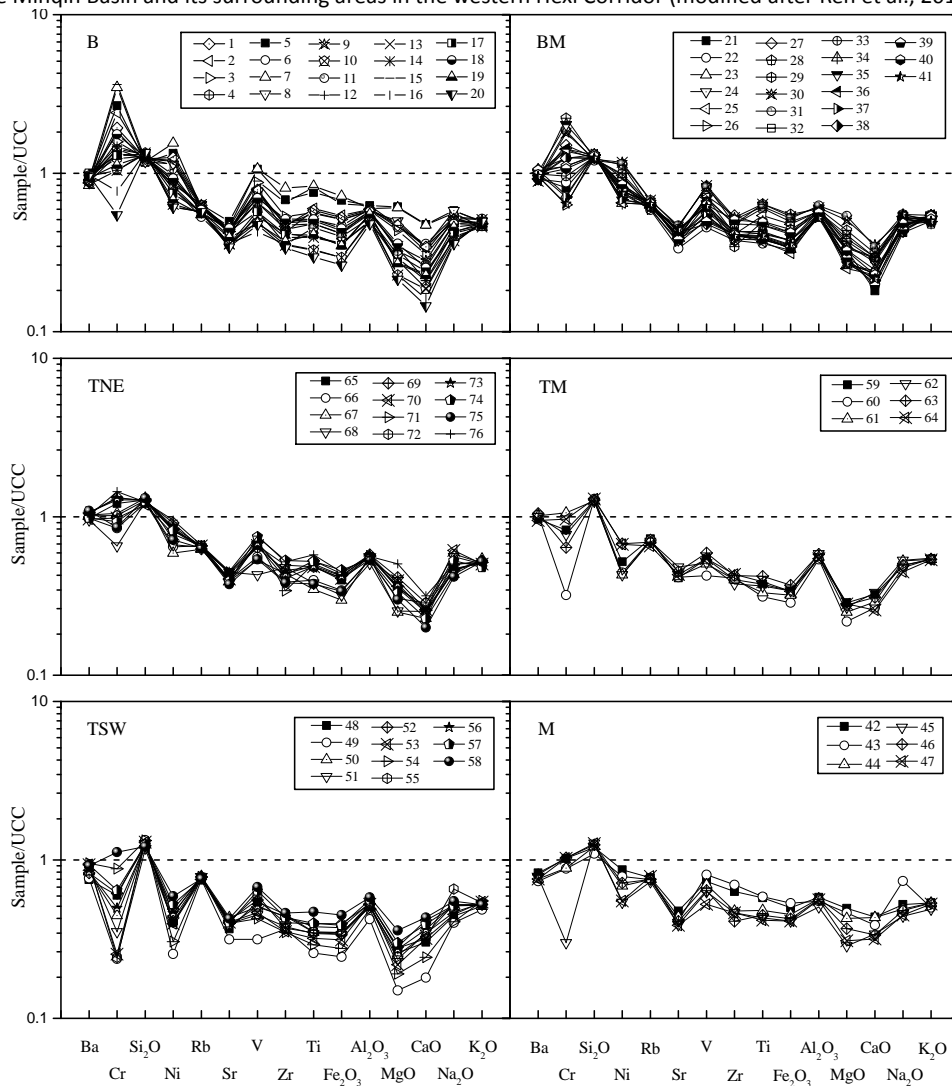


1060

1061

1062

Fig. 5 The UCC-standardized distributions and compositions of major and trace elements of sand dunes in the Minqin Basin and its surrounding areas in the western Hexi Corridor (modified after Ren et al., 2014)



1063

1064

1065

1066

1067

1068

1069

1070

1071

1072

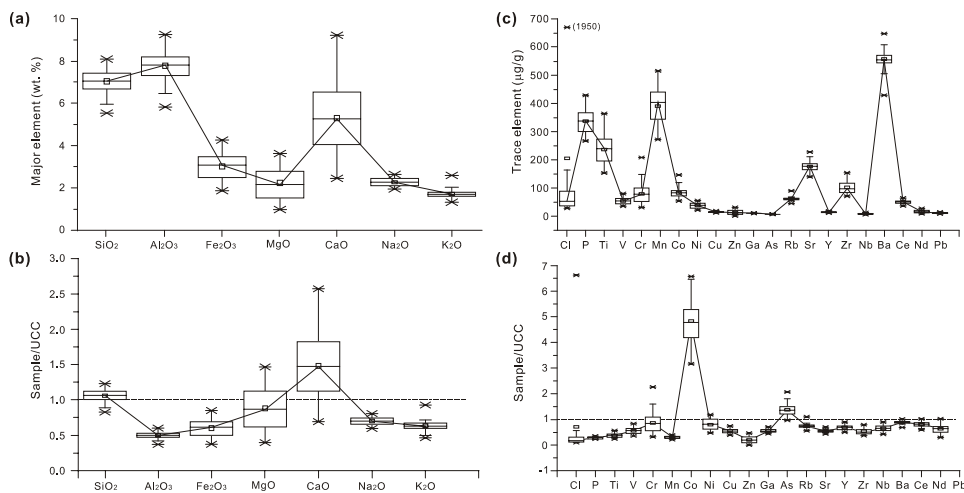
1073

1074



1075
1076
1077
1078

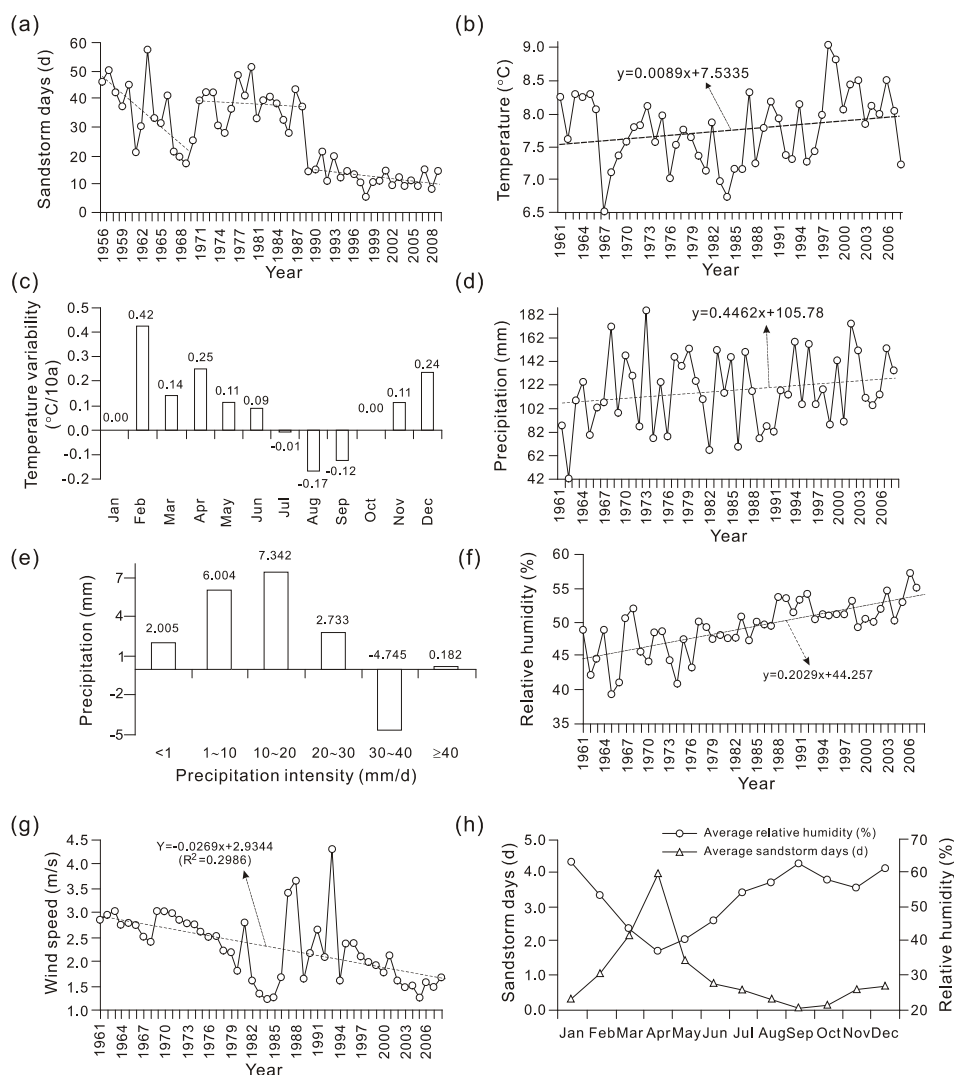
Fig. 6 Compositions of the major and trace elements and their UCC-standardized distributions of sandy dunes in the Jinta-Gaotai area of the middle Hexi Corridor (modified after Zhang et al., 2020)



1079
1080
1081
1082
1083
1084
1085
1086
1087
1088
1089
1090
1091
1092
1093
1094
1095
1096
1097
1098
1099
1100
1101
1102
1103
1104
1105
1106
1107
1108
1109



1110
 1111 Fig. 7 Changes of climate parameters in Hexi Corridor in recent 50 years (modified after Chang et al., 2011).
 1112 (a) Variation of annual average temperature during 1961-2008 in Minqin; (b) Temperature variability
 1113 during 1961-2008 in Minqin; (c) Variation of annual mean precipitation during 1961-2008 in Minqin; (d)
 1114 Variation and distribution of precipitation intensity during 1961-2008 in Minqin; (e) Variation of annual
 1115 relative air humidity during 1961-2008 in Minqin; (f) Variation of annual average wind speed during
 1116 1961-2008 in Minqin; (g) Variation of sandstorm days during 1956-2008 in Minqin; (h) Comparison of the
 1117 monthly average sandstorm days and the monthly average relative air humidity during 1961-2008 in
 1118 Minqin.

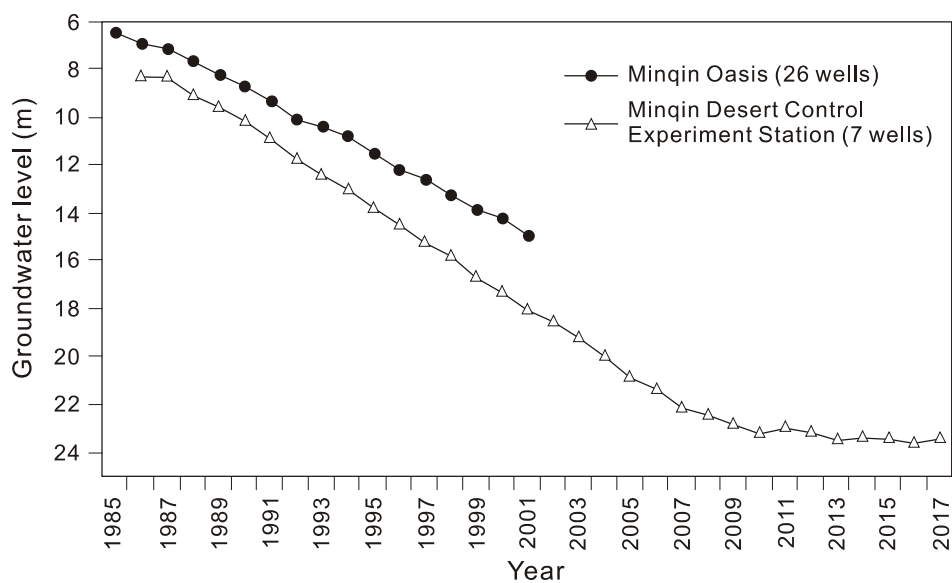


1119
 1120
 1121
 1122
 1123
 1124



1125
1126

Fig. 8 Variational trend of groundwater levels in the Minqin area (modified after Chang, 2019)



1127
1128
1129
1130
1131



1132
 1133
 1134

Tables and Table Captions:

Table 1 the locations, heights, movement directions, and lengths of dunes in the Hexi Corridor

Dune type	Dune ID	Geographic location		Height of dunes (m)	Movement direction (N-W)	Length of the beaches (m)		Source
		Longitude (E)	Latitude (N)			Upwind	Downwind	
Barchan dunes	1	102°55'16"	38°37'52"	9.8	48°	438.5	252	Chang et al., 2016a, 2017
	2	102°55'13"	38°38'00"	11.2	48	163.3	492.7	Chang et al., 2016a, 2017
	3	102°55'05"	38°36'06"	9.5	48°	129.2	163.3	Chang et al., 2016a, 2017
	4	102°55'02"	38°37'51"	3.7	48°	304.2	484.1	Chang et al., 2016a, 2017
	5	102°56'34"	38°32'11"	7.9	45°	271.7	229.4	Chang et al., 2016a, 2017
	6	102°56'43"	38°31'59"	7.6	46°	762.3	430.1	Chang et al., 2016a, 2017
	7	102°54'37"	38°25'47"	3.9	45°	295.9	80.8	Chang et al., 2016a, 2017
	8	102°52'56"	38°25'17"	5.9	87°	42.6	52	Chang et al., 2016a, 2017
	9	98°49'44"	39°57'41"	5	51°	350.4	254.5	Chang et al., 2016a, 2017
	10	98°49'59"	39°58'07"	2.6	54°	222.8	437.9	Chang et al., 2016a, 2017
	11	98°49'18"	40°00'41"	7.2	57°	184.6	197.3	Chang et al., 2016a, 2017
Chains of barchans dunes	12	102°54'53"	38°37'46"	6.4	54°	726.9	752.8	Chang et al., 2016a, 2017
	13	102°55'55"	38°37'48"	5.8	54°	443.4	406.7	Chang et al., 2016a, 2017
	14	102°54'46"	38°37'24"	11.1	50°	794.8	658.4	Chang et al., 2016a, 2017
	15	98°51'17"	39°57'59"	13.8	53°	413.6	361.1	Chang et al., 2016a, 2017
	16	98°51'31"	39°57'31"	8.7	54°	501.8	466.2	Chang et al., 2016a, 2017
	17	98°48'04"	39°58'50"	9.6	53°	554	445	Chang et al., 2016a, 2017
Pyramid dunes	18	94°42'23"	40°05'16"	25.8	SW-NE	/	/	Chang et al., 2016a, 2017
	19	94°42'10"	40°05'14"	90.3	SW-NE	/	/	Chang et al., 2016a, 2017
	20	94°41'47"	40°05'11"	76.6	SW-NE	/	/	Chang et al., 2016a, 2017
	21	94°40'53"	40°05'11"	121.8	SW-NE	/	/	Chang et al., 2016a, 2017



	22	94°40'43"	40°05'09"	114.1	SW-NE	/	/	Chang et al., 2016a, 2017
	23	94°40'12"	40°05'24"	88.9	SW-NE	/	/	Chang et al., 2016a, 2017
Parabolic dunes	24	102°57'15"	38°36'27"	4.6	/	286.1	35.3	Chang et al., 2016a, 2017
	25	102°57'42"	38°36'26"	4.4	/	228.9	188	Chang et al., 2016a, 2017
	26	102°58'15"	38°36'10"	3.3	/	133.3	198.5	Chang et al., 2016a, 2017
	27	93°59'40"	38°37'08"	3.7	/	396	302.2	Chang et al., 2016a, 2017
	28	98°41'36"	41°35'64"	4.4	/	59.9	0	Chang et al., 2016a, 2017
	29	98°41'20"	40°08'51"	4.1	/	15.7	17.7	Chang et al., 2016a, 2017
Accumulated sand-belts (longitudinal dunes belts)	30	103°12'36"	38°47'57"	15.2	/	70.4	farmland	Chang et al., 2016a, 2017
	31	103°13'30"	38°48'36"	17.1	/	44	farmland	Chang et al., 2016a, 2017
	32	103°32'03"	39°02'12"	18.6	/	811.7	farmland	Chang et al., 2016a, 2017
	33	103°31'29"	39°02'10"	5.6	/	707.7	farmland	Chang et al., 2016a, 2017
	34	103.29'49"	39°02'34"	12.2	/	1557.6	farmland	Chang et al., 2016a, 2017
	35	103°26'19"	39°02'20"	9.4	/	207.1	223.4	Chang et al., 2016a, 2017

1135

1136 Table 2 Morphological characteristics of barchans dunes in the Hexi Corridor

Dune ID	Plots area	Height (m)	Thickness of camponotus (m)	Length (m)	Width (m)	Slope of leeward direction (°)	Forward direction (°)	Beach land length of upwind (m)	Beach land length of downwind (m)	Source
1	Minqin 3-1	9.8	123.3	214.6	202.5	32.6	N48°W	662.9	378	Chang et al., 2017
2	Minqin 3-2	11.2	155.7	294.4	227.4	32.2	N48°W	163.3	491.6	Chang et al., 2017
3	Minqin 3-3	9.5	12.5	197.5	209.8	32.1	N48°W	134.2	176.6	Chang et al., 2017
4	Minqin L	3.7	78.8	86.5	81.8	31.8	N48°W	251.8	367.8	Chang et al., 2017
5	Minqin 9	7.9	90.8	112.5	81.5	32.9	N45°W	214.3	253.3	Chang et al., 2017
6	Minqin 10	7.6	86.7	136.8	64.7	31.5	N46°W	137.9	430.1	Chang et al., 2017



7	Minqin 11	11.6	104.4	183.6	57.3	31.6	N46°W	179.9	243.1	Chang et al., 2017
8	Minqin 12	8.6	64.1	131.4	77.9	30.1	N46°W	135.2	697.3	Chang et al., 2017
9	Jinchang 1	8.4	130.3	197.6	123.2	31.7	N55°W	227.4	372.1	Chang et al., 2017
10	Jingta 1	6	83.7	125.3	104.8	31.5	N63°W	250.4	129.5	Chang et al., 2017
11	Jinta 2	5.3	73.5	104.8	76.6	31.7	N63°W	108.2	419.8	Chang et al., 2017

1137
 1138
 1139

Table 3 The average element contents (%) of sandy dunes in the Hexi Corridor and other deserts and the average composition of the upper continental crust (UCC). CLP, the Loess Plateau in China.

Regions	Fe ₂ O ₃	CaO	MgO	SiO ₂	Al ₂ O ₃	Na ₂ O	K ₂ O	References
Hexi Corridor	3.5	5.55	2.07	66.12	9.24	2.45	2	Zhang et al., 2017; Pan et al., 2019
Badanjilin Desert	1.93	2.06	1.19	80.27	7.78	1.9	2	Zhu and Yang, 2009
Tenggeli Desert	1.96	1.3	1.12	80.94	8.026	1.88	2.25	Zhu and Yang, 2009
Kumutage Desert	2.88	4.64	2.19	70.13	9.59	2.52	1.98	Dong et al., 2011
Taklamakan Desert	3.1	7.88	2.2	62.05	10.6	2.58	2.11	Zhu and Yang, 2009
Loess (CLP)	4.56	8.62	2.31	58.65	11.86	1.68	2.44	Dong et al., 2011
paleosol (CLP)	5.12	0.83	2.21	65.18	14.79	1.41	3.15	Dong et al., 2011
UCC	5	4.2	2.22	66	15.2	3.9	3.4	Taylor and McLennan, 1985
Terrestrial shale	7.22	1.3	1.2	62.8	18.9	1.2	3.7	Taylor and McLennan, 1985

1140
 1141

Table 4 Meteorological data of sandstorm and strong wind in the Hexi Corridor (cited from Chang et al., 2015)

Weahter Station	Average wind speed (m/s)	Wind speed ≥ 8 grade/d	Sandstorm days (d)	Maximum wind direction
Gulang	3.5	4.5	4	NW
Wuwei	1.8	9.7	4.8	NW
Minqin	2.7	25.1	27.4	NW
Jinchang	3.3	25.1	27.4	NW
Yongchang	3	24.6	4.2	NW
Zhangye	2	12.2	11.8	NNW



Linze	2.5	21.7	7.7	NW
Gaotai	2	7.8	11.1	NW
Jiuquan	2.2	16.6	10.3	NNW
Jinta	1.9	14.4	6.4	NW, WNW
Yunmen	3.8	40.6	8.1	WNW
Average	2.61	18.39	11.2	/

1142

1143 Table 5 Changes in the area of the sand-fixing forest in different years in the Minqin Basin (cited from Chang, 2019)

Year	Planted forest								Natural forest					
	Arbor forest		Shrub forest						Nitraria tangutorum earth bags with different coverages			Chinese Tamarisk earth bags	Korshinsk Peashrub	euphrates poplar
	Elaeagnus angustifolia	other	Haloxylon ammodendron	Hedysarum scoparium	Korshinsk Peashrub	Salix glabra	Chinese Tamarisk	other	≥ 0.4	< 0.3	< 0.1			
1981	16840	855.9	13044	171.8	19	690.9	227.7	4	23379	36377	12662	5238	125922	372.6
2002	16700	/	44600	100	3508	/	/	132800	19560	19560	14860	5011	125922	0

1144